

A POSTERIORI ERROR ANALYSIS FOR PARABOLIC VARIATIONAL INEQUALITIES*

KYOUNG-SOOK MOON¹, RICARDO H. NOCHETTO², TOBIAS VON PETERSDORFF³
AND CHEN-SONG ZHANG³

Abstract. Motivated by the pricing of American options for baskets we consider a parabolic variational inequality in a bounded polyhedral domain $\Omega \subset \mathbb{R}^d$ with a continuous piecewise smooth obstacle. We formulate a fully discrete method by using piecewise linear finite elements in space and the backward Euler method in time. We define an *a posteriori* error estimator and show that it gives an upper bound for the error in $L^2(0, T; H^1(\Omega))$. The error estimator is localized in the sense that the size of the elliptic residual is only relevant in the approximate non-contact region, and the approximability of the obstacle is only relevant in the approximate contact region. We also obtain lower bound results for the space error indicators in the non-contact region, and for the time error estimator. Numerical results for $d = 1, 2$ show that the error estimator decays with the same rate as the actual error when the space meshsize h and the time step τ tend to zero. Also, the error indicators capture the correct behavior of the errors in both the contact and the non-contact regions.

Mathematics Subject Classification. 58E35, 65N15, 65N30.

Received January 20, 2006.

1. INTRODUCTION

The pricing of options is of considerable importance in finance [28]. We consider the setting of the classical Black-Scholes model [3]: assume that the price $S(t)$ of the underlying risky asset (*e.g.*, a stock) is described by geometric Brownian motion with volatility $\alpha > 0$ and interest rate $r > 0$. An *American put option* with strike price K and expiration date T gives the holder the right to sell one asset at *any time* t before the expiration date at price K . At the time t when the option is exercised, its value is given by $H(S(t))$ with the payoff function $H(S) = (K - S)_+ = \max\{K - S, 0\}$. The problem we want to solve is the following: If at time t we have an asset price $S(t)$, what is the fair price $V(S, t)$ of the option? And when is the optimal time to exercise the option?

Keywords and phrases. *A posteriori* error analysis, finite element method, variational inequality, American option pricing.

* Partially supported by NSF Grants DMS-0204670 and DMS-0505454.

¹ Department of Mathematics and Information, Kyungwon University, Bokjeong-dong, Sujeong-gu, Seongnam-si, Gyeonggi-do, 461-701, Korea. ksmoon@kyungwon.ac.kr

² Department of Mathematics and Institute for Physical Science and Technology, University of Maryland, College Park, MD 20742, USA. rhn@math.umd.edu

³ Department of Mathematics, University of Maryland, College Park, MD 20742, USA. tvp@math.umd.edu;
zhangcs@math.umd.edu

© EDP Sciences, SMAI 2007

Under the standard assumption of a frictionless market without arbitrage one can formulate this problem as an optimal stopping problem and find that the solution $V(S, t)$ satisfies a parabolic variational inequality problem. Using the time to maturity $\tilde{t} = T - t$ and $x = \log S$ as independent variables, the function $u(x, \tilde{t}) := V(e^x, T - \tilde{t})$ satisfies the following differential inequality (we will write t instead of \tilde{t} from now on):

$$\frac{\partial u}{\partial t} + \mathcal{L}u = \frac{\partial u}{\partial t} - \frac{\alpha^2}{2} \frac{\partial^2 u}{\partial x^2} + \left(\frac{\alpha^2}{2} - r \right) \frac{\partial u}{\partial x} + ru \geq 0 \quad \text{for } x \in \mathbb{R} \text{ and } 0 < t < T \tag{1.1}$$

with the obstacle constraint

$$u(x, t) \geq \chi(x) \quad \text{for } x \in \mathbb{R} \text{ and } 0 < t < T \tag{1.2}$$

and the initial condition

$$u(x, 0) = u_0(x) = H(e^x) = \max(K - e^x, 0) \quad \text{for } x \in \mathbb{R} \tag{1.3}$$

where $\chi(x) = u_0(x)$ is the payoff function in the log of the asset price. Moreover, for each point $(x, t) \in \mathbb{R} \times (0, T)$ either (1.1) or (1.2) is an equality, which is the so-called *complementarity condition*. The set of points $\mathcal{C} := \{(x, t) \in \mathbb{R} \times (0, T) : u(x, t) = \chi(x)\}$ is called the *contact set*, and its complement \mathcal{N} the *non-contact set*. The boundary \mathcal{F} between the two sets is called the *free boundary*. The optimal stopping time t_* (*i.e.* the optimal time to exercise the option) is given by

$$t_* = \inf \{t \in [0, T] : (\log S(t), t) \in \mathcal{C}\}. \tag{1.4}$$

That means t_* is the first time when the graph of $\log S(t)$ crosses the free boundary \mathcal{F} . The solution $u(x, t)$ has a singular behavior in both time and space close to $t = 0$ and $x = \log K$ (*i.e.*, time close to maturity and price close to strike price).

This problem has to be solved on the whole real line. For practical computations one uses a bounded interval $\Omega := (-R, R)$ and boundary conditions $u(-R, t) = \chi(-R)$, $u(R, t) = 0$. This causes an error which decreases exponentially in R , and is therefore negligible for R large enough. By subtracting a suitable function from $u(x)$ we can obtain a problem with zero Dirichlet conditions and a right-hand side function f . The resulting problem is formulated variationally in $\Omega \times [0, T]$ in terms of the bilinear form

$$a(v, w) := \int_{\Omega} \left[\frac{\alpha^2}{2} v'(x)w'(x) + \left(\frac{\alpha^2}{2} - r \right) v'(x)w(x) + rv(x)w(x) \right] dx \quad \forall v, w \in H_0^1(\Omega). \tag{1.5}$$

However, in finance one also needs to consider baskets of assets with prices S_1, \dots, S_d which lead to a parabolic variational inequality for $u(x, t)$ with $x \in \mathbb{R}^d$ and bilinear form $a(\cdot, \cdot)$ and operator \mathcal{L} given by

$$a(v, w) := \langle \mathcal{L}v, w \rangle, \quad \mathcal{L}v := -\operatorname{div}(\mu^2 \nabla v) + \mathbf{b} \cdot \nabla v + cv \quad \forall v, w \in H_0^1(\Omega), \tag{1.6}$$

where $\langle \cdot, \cdot \rangle$ denotes either the L^2 scalar product or the duality pairing between $H^{-1}(\Omega)$ and $H_0^1(\Omega)$. Note that the bilinear form $a(\cdot, \cdot)$ is nonsymmetric: for $d = 1$ it is possible to symmetrize the problem but this is not always the case for $d > 1$. Therefore we are interested in variational inequalities in $\Omega \subset \mathbb{R}^d$ for a nonsymmetric operator \mathcal{L} . We allow variable coefficients μ, \mathbf{b}, c , so that we can have volatilities depending on the underlying asset prices. A weak solution of the corresponding parabolic variational inequality is a function $u(x, t)$ in $C([0, T]; L^2(\Omega)) \cap L^2(0, T; H^1(\Omega))$ such that

$$\langle \partial_t u, u - v \rangle + a(u, u - v) \leq \langle f, u - v \rangle \quad \forall v \in \mathcal{K}(t) := \{v \in H_0^1(\Omega) : v \geq \chi(t)\} \quad \text{a.e. } t \in [0, T] \tag{1.7}$$

and $u(t) \in \mathcal{K}(t)$ *a.e.* $t \in [0, T]$. Here instead of restricting ourselves to the problem (1.1), we consider a more general right-hand side function $f \in L^2(0, T; L^2(\Omega))$.

Several numerical methods have been proposed to approximate this problem for $d = 1$; among them are lattice methods, Monte Carlo methods, finite difference methods and finite element methods (see [6, 15, 28] and the references therein). In the special case of the classical American option for one asset there exist various analytic results and specialized numerical methods [13]. For $d > 1$, variational inequality (1.7) is usually solved by a finite element (or finite difference) discretization in space, and a backward Euler discretization in time. We refer to the monograph by Glowinski [12] and the references therein for a survey of numerical methods for parabolic variational inequalities.

There are a number of *a priori* error estimates available for the parabolic variational inequality (1.7), such as Johnson [14], Fetter [10], and Vuik [27], but they all assume a certain amount of regularity not valid in our setting. For instance, Johnson assumes that $u_0 \in W_\infty^2(\Omega)$, and $\chi = 0$, and obtains for \mathcal{L} symmetric (with some additional regularity assumptions) an error estimate $\mathcal{O}((\log \tau^{-1})^{1/4} \tau^{3/4} + h)$ for the $L^2(0, T; H^1(\Omega))$ error. In option pricing problems, however, the obstacle χ in (1.2) and the initial condition u_0 in (1.3) are merely Lipschitz, thereby giving rise to a solution u singular close to maturity time and points in space where the payoff function χ is nonsmooth; in fact, $\partial_t u$ and $\partial_{xx} u$ blow up in $L^2(\Omega)$ at t goes down toward 0 (see numerical example 5.4). Therefore, the *a priori* error analysis does not provide a satisfactory description of (1.7) for realistic financial applications. This also includes variable time steps and graded meshes, which are relevant to resolve space-time singularities of u but are not discussed in [10, 14, 27] where uniform time and space mesh refinement is assumed.

The *a posteriori* error analysis is much more recent and rather intricate. To gain some insight on the difficulties involved, we let $\mathfrak{A}(u) := \mathcal{L}u + \sigma(u)$ be the nonlinear operator of (1.7), which consists of the linear nonsymmetric operator \mathcal{L} and the nonlinear part σ that accounts for the unilateral constraint $u \geq \chi$. The latter is the so-called Lagrange multiplier, and satisfies

$$\sigma(u) = 0 \quad \text{in } \mathcal{N} = \{u > \chi\}, \quad \sigma(u) = f - u_t - \mathcal{L}u \leq 0 \quad \text{in } \mathcal{C} = \{u = \chi\}; \tag{1.8}$$

hence $\sigma(u)$ restores the equality in (1.7), namely,

$$u_t + \mathcal{L}u + \sigma(u) = f. \tag{1.9}$$

A posteriori error estimates of residual type are obtained by plugging the discrete solution U into the PDE. Roughly speaking, we get the defect measure

$$\mathcal{G} = U_t + \mathcal{L}U + \sigma(U) - f, \tag{1.10}$$

which is called *Galerkin functional* in this nonlinear context; precise definitions are given in Section 2.5. This is a replacement for the usual residual in linear theory and shows that, to obtain sharp *a posteriori* error estimators, we must be able to provide a discrete multiplier $\sigma(U)$ with properties similar to (1.8). In fact, the linear part \mathcal{R} of \mathcal{G} , that is $\mathcal{R} := U_t + \mathcal{L}U - f$, does not give correct information in the contact set \mathcal{N} , where the solution adheres to the obstacle regardless of the size of \mathcal{R} .

Our analysis hinges on the following two key ideas, both about dealing with $\sigma(u)$:

- *Time discretization:* The nonlinear operator $\mathfrak{A}(u) = \mathcal{L}u + \sigma(u)$ of (1.7) is angle-bounded (see Sect. 2.2). This allows for optimal order-regularity error estimates for the implicit Euler method with variable time steps, as shown by Nchetto *et al.* [17, 18]. Notice the importance of exploiting the structure of $\sigma(u)$ because its dependence on u is not smooth.
- *Space discretization:* A suitable definition of discrete contact and non-contact sets (see Sect. 2.3), as well as a discrete Lagrange multiplier $\sigma(U)$ (see Sect. 2.4), inspired by those of Fierro and Veerer [11]. This yields a space error estimator which is localized in that the estimator vanishes in the discrete contact set, except for obstacle resolution, whereas it reduces to the linear residual \mathcal{R} in the discrete non-contact set where obstacle resolution is immaterial.

We point out that failure to recognize the importance of $\sigma(u)$ leads to a global upper bound of the error but not to a global lower bound [8]; overestimation is thus possible. This issue was first addressed for elliptic variational inequalities by Veerer [23] and further improved by Fierro and Veerer [11] in $H^1(\Omega)$. Nochetto *et al.* extended these estimates to $L^\infty(\Omega)$ and derived barrier set estimates [19, 20]. If the variational inequality becomes an equality, our *energy* estimates reduce to those in [2, 21, 25]. The *duality* approach, reported in [1], is not suitable in this setting because of the singular character of $\sigma(u)$.

In this paper we construct, analyze, and test a computable *a posteriori* error estimator of residual type for a full discretization of (1.7), consisting of continuous piecewise linear finite elements in space and the implicit Euler method in time, under realistic regularity assumptions. This undertaking is critical in finance but seems to be missing in the literature. Our main result is an *a posteriori* upper bound (up to a multiplicative constant) for the error in the $L^2(0, T; H^1(\Omega))$ -norm. We also obtain lower bounds for the error in terms of the leading term of the space error estimator in the non-contact region and the time error estimator. This means that the space error estimator as well as the time error estimator must decay with the correct rate. Moreover, the space error estimator is a sum of local terms which are bounded from below by the local actual error. Therefore these local terms are suitable as indicators for refinement in an adaptive method. Similarly, the time estimator is a sum of terms for each time step which can be used as indicators for refinement of the time step. We do not pursue this endeavor here.

In our numerical experiments of Section 5, we measure the error in $L^2(0, T; H^1(\Omega))$. Our results indicate that the time and space components of the error as well as the error estimator indeed converge with the expected rates. For *smooth initial data*, and uniform meshes in space and time with meshsizes τ and h , respectively, we obtain an optimal convergence rate of $\mathcal{O}(\tau + h)$; see Sections 5.2 and 5.6. In the case of *nonsmooth initial data*, the convergence rate is suboptimal but the ratio between total error estimator and error is close to a moderate constant. For the American option pricing problem with initial condition u_0 given by (1.3), thus almost in $H^{\frac{3}{2}}(\Omega)$, we obtain a suboptimal rate $\mathcal{O}(\tau^{3/4})$ for both the total error estimator and the time error estimator. Because of the expected asymptotic solution behavior at $t \rightarrow 0$, we can compensate for this with an (*a priori*) graded time partition, and thereby obtain an error estimator which converges with optimal rate $\mathcal{O}(\tau + h)$; see Section 5.4. The same strategy can be used in several space dimensions $d > 1$ for a continuous, piecewise smooth payoff function $\chi(x)$. In the case when the space mesh does not resolve the obstacle χ in the contact region, we observe that both the obstacle consistency error estimator and true error decay with the same suboptimal rate. Using appropriate local refinement, we can recover the optimal rates for both true error and error estimator; see Section 5.3.

The outline of the paper is as follows. In Section 2 we introduce the parabolic variational inequality and the corresponding discrete problem. Since the underlying operator is angle-bounded, we review the definition and properties as well. We also define the discrete non-contact set and full-contact set, and the discrete Lagrange multipliers which play a key role in the construction of the error estimator. In Section 3 we present the error estimator for a time independent piecewise linear obstacle χ and prove that it gives an upper bound of the actual error in $L^2(0, T; H^1(\Omega))$. We also prove that the space and time error estimator terms are lower bounds of the actual error. In Section 4 we consider obstacles χ that are not contained in the finite element space and give an upper bound with additional terms resulting from the obstacle approximation, the so-called obstacle consistency terms. In Section 5 we present several numerical results for $d = 1$ and $d = 2$ including American option problem, and compare the behavior of error and estimators. We finally summarize our conclusions in Section 6.

2. VARIATIONAL FORMULATION

Throughout this paper we use the following notation. For $\omega \subset \Omega$, we denote by $\langle \cdot, \cdot \rangle_\omega$ the inner product in $L^2(\omega)$ or the duality pairing between $H^{-1}(\omega)$ and $H_0^1(\omega)$, and by $\|\cdot\|_\omega := \langle \cdot, \cdot \rangle_\omega^{\frac{1}{2}}$ the corresponding norm. We also employ the energy norm $\|\cdot\|_\omega$ induced by the operator \mathcal{L} as well as its dual norm $\|\cdot\|_{*,\omega}$; see (2.3). We omit

the subscript ω provided $\omega = \Omega$ and no confusion arises. Finally, the symbol $A \lesssim B$ means $A \leq CB$ with a constant C independent of space meshsize h and time step τ , and $A \approx B$ abbreviates $A \lesssim B \lesssim A$.

2.1. Continuous and discrete problems

Let Ω be an open bounded polyhedron domain in \mathbb{R}^d and $\mathcal{Q} := (0, T) \times \Omega$ be the parabolic cylinder with lateral boundary $\Gamma := (0, T) \times \partial\Omega$. Consider an obstacle $\chi \in H^1(\mathcal{Q})$ such that $\chi \leq 0$ on Γ and nonempty convex sets

$$\mathcal{K}(t) := \{v \in H_0^1(\Omega) : v \geq \chi(t)\} \quad \text{a.e. } t \in [0, T], \tag{2.1}$$

where $H_0^1(\Omega)$ is the usual Sobolev space of function with square integrable weak derivatives and vanishing trace. If $H^{-1}(\Omega)$ denotes the dual space of $H_0^1(\Omega)$, we consider the linear operator $\mathcal{L} : H_0^1(\Omega) \rightarrow H^{-1}(\Omega)$ given by

$$\mathcal{L}v := -\text{div}(\mu^2 \nabla v) + \mathbf{b} \cdot \nabla v + cv \tag{2.2}$$

with coefficients $\mu^2 \in L^\infty(\Omega)$, $\mathbf{b} \in [W^{1,\infty}(\Omega)]^d$, $c \in L^\infty(\Omega)$ satisfying

$$\mu^2(x) \geq \mu_0^2 > 0, \quad \|\mathbf{b}(x)\| \leq b_0, \quad \rho(x) := -\frac{1}{2} \text{div } \mathbf{b}(x) + c(x) \geq \rho_0^2 \geq 0 \quad \text{a.e. } x \in \Omega,$$

for some nonnegative constants μ_0, b_0, ρ_0 . Such an operator induces the *energy norm*

$$\|v\|_\omega := \langle \mathcal{L}v, v \rangle_\omega^{\frac{1}{2}} = \left(\int_\omega \mu^2 |\nabla v|^2 + \rho |v|^2 dx \right)^{\frac{1}{2}} \quad \forall v \in H_0^1(\omega), \tag{2.3}$$

as well as the dual norm $\|\cdot\|_{*,\omega} := \sup_{v \in H_0^1(\Omega)} \langle \cdot, v \rangle_\omega / \|v\|_\omega$. It is easy to check that $\|\cdot\|_\omega$ and $\|\cdot\|_{*,\omega}$ are equivalent to the norms in $H_0^1(\omega)$ and $H^{-1}(\omega)$, respectively. The operator \mathcal{L} also gives rise to the continuous and coercive bilinear form $a(\cdot, \cdot) : [H_0^1(\Omega)]^2 \rightarrow \mathbb{R}$ defined by

$$a(v, w) := \int_\Omega \mu^2 \nabla v \cdot \nabla w + (\mathbf{b} \cdot \nabla v)w + cvw \quad \forall v, w \in H_0^1(\Omega).$$

We then consider the following continuous parabolic variational inequality:

Problem 2.1. Let $\mathcal{K}(t)$ be the convex sets defined in (2.1) and $u_0 \in \mathcal{K}(0)$. Given data $f \in L^2(0, T; L^2(\Omega))$, find $u \in C([0, T]; L^2(\Omega)) \cap L^2(0, T; H^1(\Omega))$ such that

$$\langle \partial_t u, u - v \rangle + a(u, u - v) \leq \langle f, u - v \rangle, \quad \forall v \in \mathcal{K}(t) \quad \text{a.e. } t \in [0, T] \tag{2.4}$$

and

$$u(t) \in \mathcal{K}(t) \quad \text{a.e. } t \in [0, T]$$

with initial condition $u(0, x) = u_0(x)$ in Ω and boundary condition $u(t, x) = 0$ on Γ for a.e. $t \in [0, T]$ (see [4], Chap. III).

For the numerical treatment of this problem, we discretize the spatial domain Ω into simplexes $S \in \mathcal{T}_h$, and partition the time domain $[0, T]$ into N subintervals, i.e. $0 = t_0 < t_1 < \dots < t_N = T$ and let $\tau_n := t_n - t_{n-1}$. Let h_S be the diameter of $S \in \mathcal{T}_h$ and $h(x)$ be the local meshsize, that is the piecewise constant function with $h|_S := h_S$ for all $S \in \mathcal{T}_h$. Given a node z , we set $h_z := \max\{\text{diam}(S) : S \in \mathcal{T}_h \text{ and } z \in S\}$.

Let \mathbb{V}_h be the usual conforming piecewise linear finite element subspace of $H_0^1(\Omega)$ over the mesh \mathcal{T}_h . In this paper, we assume that meshes do not change in time. Mesh adaptation as well as the design of adaptive algorithms will be considered in [16]. Consider the corresponding discrete convex set

$$\mathcal{K}_h^n := \{v \in \mathbb{V}_h : v \geq \chi_h^n\} \tag{2.5}$$

where the sequence $\chi_h^n \in \mathbb{V}_h$ is a piecewise linear approximation of the obstacle $\chi(t_n)$ for $0 \leq n \leq N$. For example, when the obstacle χ is continuous, we could take χ_h^n to be the piecewise linear Lagrange interpolant of $\chi(t_n)$. Now we formulate the following fully discrete numerical approximation of Problem 2.1 by using linear finite elements in space and backward Euler method in time:

Problem 2.2. *Given the approximation $F_h^n \in L^2(\Omega)$ of f at time t_n for $1 \leq n \leq N$, and initial guess $U_h^0 \in \mathcal{K}_h^0$, find an approximate solution $U_h^n \in \mathcal{K}_h^n$ for $1 \leq n \leq N$ such that*

$$\frac{1}{\tau_n} \langle U_h^n - U_h^{n-1}, U_h^n - v_h \rangle + a(U_h^n, U_h^n - v_h) \leq \langle F_h^n, U_h^n - v_h \rangle, \quad \forall v_h \in \mathcal{K}_h^n. \tag{2.6}$$

This problem admits a unique solution [12]. Moreover, let $\{\phi_{z_i}\}_{i=1}^I$ be the set of nodal basis functions (here $\{z_i\}_{i=1}^I$ are interior nodes), and let $A := (\langle \phi_{z_i}, \phi_{z_j} \rangle + \tau_n a(\phi_{z_i}, \phi_{z_j}))_{i,j=1}^I$ be the resulting matrix of (2.6). If $\vec{U} = (U_i), \vec{X} = (X_i) \in \mathbb{R}^I$ are the vector of nodal values of U_h^n and χ_h^n , namely $U_h^n = \sum_{i=1}^I U_i \phi_{z_i}$ and $X_h^n = \sum_{i=1}^I X_i \phi_{z_i}$, and $\vec{F} = (\langle U_h^{n-1} + \tau_n F_h^n, \phi_{z_i} \rangle)_{i=1}^I = (F_i)$, then \vec{U} satisfies the *complementarity* system:

$$A\vec{U} \geq \vec{F}, \quad \vec{U} \geq \vec{X}, \quad (A\vec{U} - \vec{F})^T (\vec{U} - \vec{X}) = 0. \tag{2.7}$$

Therefore, the equality $(A\vec{U})_i = F_i$ holds at every node z_i where $U_i > X_i$. This leads to the notion of non-contact node defined in Section 2.3.

2.2. Angle-bounded operators

A linear monotone operator $\mathcal{L} : H_0^1(\Omega) \rightarrow H^{-1}(\Omega)$ is called *sectorial* if it satisfies the *strong sector* condition

$$|\langle \mathcal{L}v, w \rangle|^2 \leq 4\gamma^2 \|v\|^2 \|w\|^2 \quad \forall v, w \in H_0^1(\Omega). \tag{2.8}$$

This is equivalent to the following inequality for the skew-symmetric part of \mathcal{L} [5], Proposition 11:

$$|\langle \mathcal{L}v, w \rangle - \langle \mathcal{L}w, v \rangle| \leq 2\lambda \|v\| \|w\| \quad \forall v, w \in H_0^1(\Omega), \tag{2.9}$$

with a positive constant λ satisfying $\gamma^2 = (\lambda^2 + 1)/4$. We observe that (2.8) implies that \mathcal{L} is Lipschitz continuous and $\|\mathcal{L}v\|_* = \sup_{w \in H_0^1(\Omega)} \langle \mathcal{L}v, w \rangle / \|w\|$ satisfies

$$\frac{1}{4\gamma^2} \|\mathcal{L}v\|_*^2 \leq \|v\|^2 \leq \|\mathcal{L}v\|_*^2 \quad \forall v \in H_0^1(\Omega).$$

We are now ready to recall the notion of *angle-bounded operator*. This was introduced by Brézis and Browder [5] as a nonlinear generalization of sectorial operators, and more recently revisited by Caffarelli in the context of regularity theory [7].

Definition 2.3. Let \mathcal{H} be a Hilbert space, and let $D(\mathfrak{A}) \subset \mathcal{H}$ be the domain of an operator $\mathfrak{A} : \mathcal{H} \rightarrow 2^{\mathcal{H}}$. Then \mathfrak{A} is said to be γ^2 -angle-bounded if there exists a positive constant γ such that

$$\langle \mathfrak{A}(v) - \mathfrak{A}(w), w - z \rangle \leq \gamma^2 \langle \mathfrak{A}(v) - \mathfrak{A}(z), v - z \rangle \quad \forall v, w, z \in D(\mathfrak{A}). \tag{2.10}$$

Lemma 2.4 (equivalence). *The conditions (2.8) and (2.10) are equivalent for \mathcal{L} linear.*

Proof. We simply set $\tilde{v} = v - z$ and $\tilde{w} = w - z$ in (2.10) to get the equivalent formulation (we omit the tildes)

$$\langle \mathcal{L}v, w \rangle \leq \gamma^2 \langle \mathcal{L}v, v \rangle + \langle \mathcal{L}w, w \rangle \quad \forall v, w \in D(\mathcal{L}). \tag{2.11}$$

Then replace v by αv with $\alpha \in \mathbb{R}$ and argue with the resulting quadratic inequality in α to realize that (2.8) and (2.11) are equivalent. □

Lemma 2.5 (\mathcal{L} is sectorial). *The operator \mathcal{L} defined in (2.2) is sectorial with constant γ given by*

$$\gamma^2 = \frac{1}{4} \left(1 + \frac{b_0^2}{\mu_0^2(\rho_0^2 + \mu_0^2 P_0^2)} \right), \tag{2.12}$$

where P_0 is the constant in the Poincaré inequality $P_0 \|v\| \leq \|\nabla v\|$ for all $v \in H_0^1(\Omega)$.

Proof. This proof hinges on (2.9). Since

$$\|v\|^2 \geq \mu_0^2 \|\nabla v\|^2, \quad \|v\|^2 \geq (\rho_0^2 + \mu_0^2 P_0^2) \|v\|^2 \quad \forall v \in H_0^1(\Omega),$$

the skew-symmetric part of \mathcal{L} satisfies for all $v, w \in H_0^1(\Omega)$

$$|\langle \mathcal{L}v, w \rangle - \langle \mathcal{L}w, v \rangle| \leq b_0 \|\nabla v\| \|w\| + b_0 \|\nabla w\| \|v\| \leq \frac{2b_0}{\mu_0(\rho_0^2 + \mu_0^2 P_0^2)^{\frac{1}{2}}} \|v\| \|w\|,$$

whence $\lambda = b_0 \mu_0^{-1} (\rho_0^2 + \mu_0^2 P_0^2)^{-\frac{1}{2}}$. The assertion (2.12) follows from $\gamma^2 = (1 + \lambda^2)/4$ [5], Proposition 11. \square

If $\mathcal{K} = \mathcal{K}(t)$ is the convex set defined in (2.1), we let $\mathfrak{A} : \mathcal{K} \rightarrow H^{-1}(\Omega)$ be the multivalued operator associated with the variational inequality in \mathcal{K} , *i.e.*

$$v_* \in \mathfrak{A}(v) \iff a(v, v - w) \leq \langle v_*, v - w \rangle \quad \forall w \in \mathcal{K}. \tag{2.13}$$

If we further define the multivalued operator $\sigma(v) := \mathfrak{A}(v) - \mathcal{L}v$ with $D(\sigma) = \mathcal{K}$, we see that $\sigma(v) \leq 0$ in Ω and $\sigma(v) = 0$ in $\mathcal{N} = \{v > \chi(t)\}$ (simply argue with $w = v + \varphi$). It turns out that σ is the subdifferential $\partial I_{\mathcal{K}}$ of the indicator function $I_{\mathcal{K}}$ of \mathcal{K} , which is defined as zero in \mathcal{K} and ∞ in the complement. Such a σ can be viewed as a Lagrange multiplier of the constraint $v \geq \chi(t)$, an interpretation that we exploit in Section 2.4.

Lemma 2.6 (\mathfrak{A} is angle-bounded). *The operator $\mathfrak{A} = \mathcal{L} + \sigma$ is γ_0^2 -angle-bounded with constant $\gamma_0 = \max(1, \gamma)$, γ being defined in (2.12). Moreover, \mathfrak{A} satisfies for all $v, w, z \in \mathcal{K}$*

$$\begin{aligned} \langle \mathfrak{A}(v) - \mathfrak{A}(w), w - z \rangle &\leq \gamma^2 \langle \mathcal{L}v - \mathcal{L}z, w - z \rangle + \langle \sigma(v), w - z \rangle \\ &\leq \gamma^2 \langle \mathcal{L}v - \mathcal{L}z, w - z \rangle + \langle \sigma(v) - \sigma(z), w - z \rangle. \end{aligned} \tag{2.14}$$

Proof. Since $\mathfrak{A}(v) = \mathcal{L}v + \sigma(v)$, in view of Lemmas 2.4 and 2.5 we only need to deal with $\sigma(v)$. We resort to the fact that $\sigma(v) = \partial I_{\mathcal{K}}(v)$, which translates into the property

$$\langle \sigma(v), w - v \rangle \leq 0 \quad \forall v, w \in \mathcal{K}.$$

In fact, if $v > \chi(t)$ then $\sigma(v) = 0$ whereas if $v = \chi(t) \leq w$ then $\sigma(v) \leq 0$. Consequently

$$\langle \sigma(v) - \sigma(w), w - z \rangle = \langle \sigma(v), w - z \rangle + \langle \sigma(v), w - v \rangle + \langle \sigma(w), z - w \rangle \leq \langle \sigma(v), w - z \rangle \leq \langle \sigma(v) - \sigma(z), w - z \rangle,$$

whence we deduce (2.14)

$$\langle \mathfrak{A}(v) - \mathfrak{A}(w), w - z \rangle \leq \gamma^2 \langle \mathcal{L}v - \mathcal{L}w, w - z \rangle + \langle \sigma(v) - \sigma(z), w - z \rangle \leq \gamma_0^2 \langle \mathfrak{A}(v) - \mathfrak{A}(z), w - z \rangle.$$

The last inequality implies that \mathfrak{A} is γ_0 -angle-bounded, as asserted. \square

We conclude this section with the *coercivity* Lemma 4.3 of [18], which will be crucial in Section 3.1.

Lemma 2.7 (coercivity). *Let γ be defined in (2.12). The linear operator \mathcal{L} defined in (2.2) satisfies*

$$\langle \mathcal{L}v - \mathcal{L}w, w - z \rangle \leq 2\gamma^2 \|v - z\|^2 - \frac{1}{4} \left(\|v - w\|^2 + \|z - w\|^2 \right) \quad \forall v, w, z \in \mathcal{K}. \tag{2.15}$$

Proof. In view of the definition (2.3) of $\|\cdot\|$, Lemma 2.5, and Cauchy-Schwarz inequality we get

$$\begin{aligned} \langle \mathcal{L}v - \mathcal{L}w, w - z \rangle &= \langle \mathcal{L}v - \mathcal{L}w, w - v \rangle + \langle \mathcal{L}v - \mathcal{L}w, v - z \rangle \\ &\leq -\|v - w\|^2 + 2\gamma \|v - w\| \|v - z\| \\ &\leq -\frac{1}{2} \|v - w\|^2 + 2\gamma^2 \|v - z\|^2. \end{aligned}$$

Similarly, we get

$$\begin{aligned} \langle \mathcal{L}v - \mathcal{L}w, w - z \rangle &= \langle \mathcal{L}z - \mathcal{L}w, w - z \rangle + \langle \mathcal{L}v - \mathcal{L}z, w - z \rangle \\ &\leq -\|z - w\|^2 + 2\gamma \|v - z\| \|w - z\| \\ &\leq -\frac{1}{2} \|z - w\|^2 + 2\gamma^2 \|v - z\|^2. \end{aligned}$$

Adding the last two inequalities gives (2.15). □

2.3. Residuals and discrete sets

For any sequence $\{W^n\}_{n=1}^N$, we define the piecewise constant interpolant \overline{W} and the piecewise linear interpolant W as

$$\overline{W}(t) := W^n, \quad W(t) := l(t)W^{n-1} + (1 - l(t))W^n \quad \forall t \in (t_{n-1}, t_n], \quad 1 \leq n \leq N, \tag{2.16}$$

where the linear function $l(t)$ is defined by

$$l(t) := \frac{t_n - t}{\tau_n} \quad \forall t \in (t_{n-1}, t_n]. \tag{2.17}$$

We also denote by $\{\delta W^n\}_{n=1}^N$ the discrete derivative of the sequence $\{W^n\}_{n=1}^N$

$$\delta W^n := \frac{W^n - W^{n-1}}{\tau_n} \quad \forall 1 \leq n \leq N. \tag{2.18}$$

For a function w continuous in time, we let $w^n(\cdot) := w(t_n, \cdot)$ be its semi-discrete approximation and \overline{w} be defined as in (2.16).

We now introduce spatial quantities for $1 \leq n \leq N$ fixed. We define the *jump residual* J_h^n on the side $S_1 \cap S_2$ to be

$$J_h^n := -\mu^2 (\nabla U_h^n|_{S_1} \cdot \nu_1 + \nabla U_h^n|_{S_2} \cdot \nu_2) \tag{2.19}$$

where ν_i is the unit outer normal vector to the element $S_i \in \mathcal{T}_h$ for $i = 1, 2$. We also define the *interior residuals* associated with the linear operator \mathcal{L} for each element of \mathcal{T}_h

$$\widehat{R}_h^n := F_h^n - \delta U_h^n - \mathbf{b} \cdot \nabla U_h^n - cU_h^n, \quad R_h^n := F_h^n - \delta U_h^n - \mathcal{L}U_h^n = \widehat{R}_h^n + \nabla(\mu^2) \cdot \nabla U_h^n. \tag{2.20}$$

We observe that R_h^n is the usual full residual, including the second order term $\text{div}(\mu^2 \nabla U_h^n) = \nabla(\mu^2) \cdot \nabla U_h^n$, and that $\widehat{R}_h^n = R_h^n$ provided that μ is constant.

Our next task is to define discrete sets that mimic the contact and non-contact sets, \mathcal{C} and \mathcal{N} , of (1.8). This is a rather tricky endeavor because our choice is related to the definition of discrete multiplier and localization. We adopt the definition of Fierro and Veerer [11], which requires dealing with stars ω_z . They are the support of the basis functions $\{\phi_z\}_{z \in \mathcal{P}_h}$, where \mathcal{P}_h is the set of all nodes of \mathcal{T}_h , including the boundary nodes. We let γ_z be the skeleton of ω_z , namely the set of all interior sides of ω_z which contain z ; for $d = 1$ we have $\gamma_z = \{z\}$ and so $\|v\|_{\gamma_z}$ reduces to the absolute value of $v(z)$. We then split \mathcal{P}_h into three disjoint sets

$$\mathcal{P}_h = \mathcal{N}_h^n \cup \mathcal{C}_h^n \cup \mathcal{F}_h^n$$

with the non-contact nodes \mathcal{N}_h^n , full-contact nodes \mathcal{C}_h^n , and free boundary nodes \mathcal{F}_h^n defined as follows [11]:

$$\mathcal{N}_h^n := \{z \in \mathcal{P}_h : U_h^n > \chi_h^n \text{ in int } \omega_z\}, \tag{2.21a}$$

$$\mathcal{C}_h^n := \{z \in \mathcal{P}_h : U_h^n = \chi_h^n \text{ and } R_h^n \leq 0 \text{ in } \omega_z, J_h^n \leq 0 \text{ on } \gamma_z\}, \tag{2.21b}$$

$$\mathcal{F}_h^n := \mathcal{P}_h \setminus (\mathcal{N}_h^n \cup \mathcal{C}_h^n). \tag{2.21c}$$

The definition of \mathcal{N}_h^n is clear since $z \in \mathcal{N}_h^n$ if and only if $U_h^n(z) > \chi_h^n(z)$. In contrast, the definition of \mathcal{C}_h^n deserves an explanation. It is motivated by localization, that is the fact that modifying U_h^n locally in ω_z should not improve the resolution, provided $\chi_h^n = \chi(t_n)$ in ω_z . In fact, if $\mathcal{K}_z^n := \{v + U_h^n : 0 \leq v \in H_0^1(\omega_z)\}$ is the convex set of local admissible functions, then we consider the variational inequality problem

$$\text{Find } V \in \mathcal{K}_z^n : \quad \frac{1}{\tau_n} \langle V - U_h^{n-1}, V - W \rangle - a(V, V - W) \leq \langle F_h^n, V - W \rangle \quad \forall W \in \mathcal{K}_z^n.$$

We claim that the unique solution of this local problem is $V = U_h^n$ and thus local improvement of U_h^n is no longer possible. If $v = 0$, then the above variational inequality becomes

$$\langle F_h^n, w \rangle - \frac{1}{\tau_n} \langle U_h^n - U_h^{n-1}, w \rangle + a(U_h^n, w) \leq 0 \quad \forall 0 \leq w \in H_0^1(\omega_z),$$

or, after integration by parts,

$$\langle R_h^n, w \rangle_{\omega_z} + \langle J_h^n, w \rangle_{\gamma_z} \leq 0 \quad \forall 0 \leq w \in H_0^1(\omega_z).$$

This is equivalent to the requirements $R_h^n \leq 0$ in ω_z and $J_h^n \leq 0$ on γ_z in (2.21b).

2.4. Lagrange multipliers

We first recall the definition of *Lagrange multiplier* $\sigma(u)$ of (1.9) and (2.13)

$$\langle \sigma(u), \varphi \rangle := \langle f - \partial_t u - \mathbf{b} \cdot \nabla u - cu, \varphi \rangle - \langle \mu^2 \nabla u, \nabla \varphi \rangle \quad \forall \varphi \in H_0^1(\Omega), \tag{2.22}$$

as well as the properties (1.8), namely,

$$\sigma(u) = 0 \quad \text{in } \mathcal{N} = \{u > \chi\}, \quad \sigma(u) = f - u_t - \mathcal{L}u \leq 0 \quad \text{in } \mathcal{C} = \{u = \chi\}.$$

We note that in the non-contact region \mathcal{N} , where the constraint is inactive, we have $\sigma(u) = 0$, whereas in the contact region \mathcal{C} we have $\sigma(u) \leq 0$. We could thus interpret $\sigma(u)$ as a reaction to the obstacle.

It is crucial for us to mimic these continuous properties at the discrete level. A first attempt would be to define a piecewise linear function $\sigma_h^n = \sum_{z \in \mathcal{P}_h} s_z^n \phi_z$ in such a way that the nodal values s_z^n are weighted means on stars ω_z :

$$s_z^n := \begin{cases} \frac{1}{\int_{\omega_z} \phi_z} \int_{\omega_z} [\widehat{R}_h^n \phi_z - \mu^2 \nabla U_h^n \nabla \phi_z], & z \in \mathcal{P}_h \cap \Omega \\ 0, & z \in \mathcal{P}_h \cap \partial\Omega; \end{cases} \tag{2.23}$$

note that σ is zero on $\partial\Omega \cap \mathcal{N}$, which motivates us to define $s_z^n = 0$ on $\partial\Omega$. This implies

$$s_z^n \int_{\omega_z} \phi_z = \int_{\omega_z} \widehat{R}_h^n \phi_z - \mu^2 \nabla U_h^n \nabla \phi_z.$$

This definition yields $s_z^n \leq 0$ and $s_z^n = 0$ for $z \in \mathcal{N}_h^n$, and it is thus quite appropriate for \mathcal{N}_h^n but not necessarily for $z \in \mathcal{C}_h^n$. In fact, to achieve localization of the error estimator σ_h^n must equal the linear residual in ω_z for $z \in \mathcal{C}_h^n$, thereby leading to

$$\sigma_h^n = F_h^n - \delta U_h^n - \mathcal{L}U_h^n$$

in the sense of distributions in ω_z . We can blend the two competing alternatives *via* the partition of unity $\{\phi_z\}_{z \in \mathcal{P}_h}$ as proposed by Fierro and Veerer [11] and Nochetto *et al.* [20]

$$\langle \sigma_h^n, \varphi \rangle := \sum_{z \in \mathcal{P}_h} \langle \sigma_h^n, \varphi \phi_z \rangle \quad \forall \varphi \in H_0^1(\Omega), \tag{2.24}$$

where

$$\langle \sigma_h^n, \varphi \phi_z \rangle := \begin{cases} \int_{\omega_z} \widehat{R}_h^n \varphi \phi_z - \mu^2 \nabla U_h^n \nabla(\varphi \phi_z) & z \in \mathcal{C}_h^n \\ \int_{\omega_z} s_z^n \varphi \phi_z & z \in \mathcal{P}_h \setminus \mathcal{C}_h^n. \end{cases} \tag{2.25}$$

We stress that σ_h^n is not a discrete object, but its definition (2.24) guarantees that $\sigma_h^n \leq 0$ in Ω . This is a consequence of $s_z^n \leq 0$ and the sign conditions in (2.21b).

2.5. Galerkin functionals

For a linear parabolic problem $\partial_t u + \mathcal{L}u = f$ it is natural to use the distribution $f - \delta U - \mathcal{L}U$ as a defect measure of the error. This so-called residual fails to be the correct quantity for variational inequalities because it provides wrong information in the contact region. The Lagrange multiplier $\sigma = \sigma(u)$ of (2.22) restores equality

$$\langle \partial_t u + \mathcal{L}u + \sigma - f, \varphi \rangle = 0 \quad \forall \varphi \in H_0^1(\Omega),$$

and leads to the notion (1.10) of *Galerkin functional* \mathcal{G}_h , which is a nonlinear defect measure; see [11, 19, 20, 23] for elliptic variational inequalities. The precise definition of \mathcal{G}_h is as follows: $\mathcal{G}_h \in L^2(0, T; H^{-1}(\Omega))$ is the piecewise constant functional in time given by

$$\begin{aligned} \langle \mathcal{G}_h, \varphi \rangle &:= \langle \partial_t U_h + \mathcal{L}\bar{U}_h + \bar{\sigma}_h - \bar{F}_h, \varphi \rangle \\ &= \langle \partial_t(U_h - u) + \mathcal{L}(\bar{U}_h - u) + (\bar{\sigma}_h - \sigma), \varphi \rangle - \langle \bar{F}_h - f, \varphi \rangle \quad \forall \varphi \in H_0^1(\Omega). \end{aligned} \tag{2.26}$$

Note that for $1 \leq n \leq N$, the Galerkin functional \mathcal{G}_h^n satisfies

$$\langle \mathcal{G}_h^n, \varphi \phi_z \rangle = \langle \sigma_h^n - \widehat{R}_h^n, \varphi \phi_z \rangle + \langle \mu^2 \nabla U_h^n, \nabla(\varphi \phi_z) \rangle \quad \forall z \in \mathcal{P}_h, \tag{2.27}$$

whence $\langle \mathcal{G}_h^n, \varphi \phi_z \rangle = 0$ for all $z \in \mathcal{C}_h^n$. This crucial property is responsible for localization and will be instrumental in Section 3.

3. A POSTERIORI ERROR ESTIMATE: PIECEWISE LINEAR TIME-INDEPENDENT OBSTACLES

In this section we derive *a posteriori* upper and lower bounds for the error in the $L^2(0, T; H^1(\Omega))$ -norm. To simplify the presentation we assume in this section that (i) the obstacle χ is time independent, and (ii) that the obstacle is a piecewise linear function and $\chi = \chi_h$. In this case we let $\chi_h^n := \chi_h$ and have

$$\chi(t_n) = \chi_h^n = \chi_h \quad \Rightarrow \quad \mathcal{K}_h^n \subset \mathcal{K} \quad \forall n = 0, \dots, N. \tag{3.1}$$

3.1. Upper bound

Upon choosing the function $\varphi = U_h - u$ in (2.26), we get the error equation

$$\frac{1}{2} \frac{d}{dt} \|U_h - u\|^2 + \langle \mathcal{L}(\bar{U}_h - u), U_h - u \rangle + \langle \bar{\sigma}_h - \sigma, U_h - u \rangle = \langle \mathcal{G}_h, U_h - u \rangle + \langle \bar{F}_h - f, U_h - u \rangle.$$

To estimate the second and third terms on the left-hand side we would like to resort to the angle-bounded structure of $\mathfrak{A} = \mathcal{L} + \sigma$, namely Lemma 2.6. However, this is not possible because $\bar{\sigma}_h$ does not coincide with

the subdifferential $\partial I_{\mathcal{K}}(U_h)$; this is the effect of both space and time discretization. The crucial *monotonicity* property $\langle \bar{\sigma}_h - \sigma, U_h - u \rangle \geq 0$ is thus no longer valid. Therefore, we split the analysis into the linear part involving \mathcal{L} and the nonlinear part involving the multipliers, but still aim at an inequality similar to (2.14). Applying Lemma 2.7, namely taking $v = \bar{U}_h, w = u$ and $z = U_h$ in (2.15), we arrive at

$$\begin{aligned} & \frac{1}{2} \frac{d}{dt} \|U_h - u\|^2 + \frac{1}{4} \left(\|\bar{U}_h - u\|^2 + \|U_h - u\|^2 \right) \\ & \leq 2\gamma^2 \|\bar{U}_h - U_h\|^2 - \langle \bar{\sigma}_h - \sigma, U_h - u \rangle + \langle \mathcal{G}_h, U_h - u \rangle + \langle \bar{F}_h - f, U_h - u \rangle. \end{aligned}$$

Invoking the definition of dual norm $\|\cdot\|_*$, a straightforward calculation gives

$$\langle \mathcal{G}_h, U_h - u \rangle + \langle \bar{F}_h - f, U_h - u \rangle \leq 4 \|\mathcal{G}_h\|_*^2 + 4 \|\bar{F}_h - f\|_*^2 + \frac{1}{8} \|U_h - u\|^2,$$

whence

$$\begin{aligned} & \frac{d}{dt} \|U_h - u\|^2 + \frac{1}{2} \|\bar{U}_h - u\|^2 + \frac{1}{4} \|U_h - u\|^2 \\ & \leq 4\gamma^2 \|\bar{U}_h - U_h\|^2 + 8 \|\mathcal{G}_h\|_*^2 + 8 \|\bar{F}_h - f\|_*^2 - 2\langle \bar{\sigma}_h - \sigma, U_h - u \rangle. \end{aligned} \tag{3.2}$$

On the other hand, using the strong sector condition (2.8) and the triangle inequality in (2.26) yields

$$\|\partial_t(U_h - u) + (\bar{\sigma}_h - \sigma)\|_*^2 \leq 12\gamma^2 \|\bar{U}_h - u\|^2 + 3 \|\mathcal{G}_h\|_*^2 + 3 \|\bar{F}_h - f\|_*^2. \tag{3.3}$$

Combining the last two inequalities, (3.2) and (3.3), and integrating on $[0, T]$ gives

$$\begin{aligned} & \|(U_h - u)(T)\|^2 + \frac{1}{4} \int_0^T \left(\|\bar{U}_h - u\|^2 + \|U_h - u\|^2 \right) dt \\ & + \frac{1}{48\gamma^2} \int_0^T \|\partial_t(U_h - u) + (\bar{\sigma}_h - \sigma)\|_*^2 dt \leq \|U_h^0 - u_0\|^2 \\ & + \int_0^T \left(4\gamma^2 \|\bar{U}_h - U_h\|^2 - 2\langle \bar{\sigma}_h - \sigma, U_h - u \rangle + \lambda (\|\mathcal{G}_h\|_*^2 + \|\bar{F}_h - f\|_*^2) \right) dt, \end{aligned} \tag{3.4}$$

with $\lambda := 8 + \frac{1}{16\gamma^2}$ and

$$\begin{aligned} & \int_0^T \|\mathcal{G}_h\|_*^2 dt = \sum_{n=1}^N \tau_n \|\mathcal{G}_h^n\|_*^2 \\ & \int_0^T \langle \bar{\sigma}_h - \sigma, U_h - u \rangle dt = \sum_{n=1}^N \int_{t_{n-1}}^{t_n} \langle \sigma_h^n - \sigma, U_h - u \rangle dt. \end{aligned}$$

Hence, to get the desired global upper bound, we need to find an appropriate upper bound of $\|\mathcal{G}_h^n\|_*^2$ and a lower bound of $\int_{t_{n-1}}^{t_n} \langle \sigma_h^n - \sigma, U_h - u \rangle dt$ for $1 \leq n \leq N$. This is achieved in the next two lemmas.

Lemma 3.1 (upper bound of Galerkin functional). *Let the sequence $\{U_h^n\}_{n=1}^N$ be the discrete solution of the variational inequality (2.6) and the discrete Galerkin functional \mathcal{G}_h^n be defined as in Section 2.5. Then there is a constant $C_G \geq 0$, independent of the meshsize h , such that*

$$\|\mathcal{G}_h^n\|_*^2 \leq C_G \sum_{z \in \mathcal{P}_h \setminus \mathcal{C}_h^n} (\eta_z^n)^2 \quad \forall n = 1, \dots, N. \tag{3.5}$$

Here the space discretization error indicator η_z^n is defined by

$$\eta_z^n := \left\{ h_z \|J_h^n\|_{L^2(\gamma_z)}^2 + h_z^2 \left\| R_h^n - \tilde{R}_z^n \right\|_{L^2(\omega_z)}^2 \right\}^{\frac{1}{2}}, \tag{3.6}$$

with J_h^n and R_h^n defined in (2.19) and (2.20), respectively, and \tilde{R}_z^n given by

$$\tilde{R}_z^n := \begin{cases} \frac{1}{|\omega_z|} \int_{\omega_z} R_h^n, & z \in \mathcal{P}_h \cap \Omega \\ 0, & z \in \mathcal{P}_h \cap \partial\Omega. \end{cases} \tag{3.7}$$

Proof. We employ the partition of unity to write $\langle \mathcal{G}_h^n, \varphi \rangle = \sum_{z \in \mathcal{P}_h} \langle \mathcal{G}_h^n, \varphi \phi_z \rangle$ for any function $\varphi \in H_0^1(\Omega)$. We next recall (2.27), in particular $\langle \mathcal{G}_h^n, \varphi \phi_z \rangle = 0$ for $z \in \mathcal{C}_h^n$, to deduce

$$\langle \mathcal{G}_h^n, \varphi \rangle = \sum_{z \in \mathcal{P}_h \setminus \mathcal{C}_h^n} \left\{ \langle \mu^2 \nabla U_h^n, \nabla(\varphi \phi_z) \rangle_{\omega_z} - \langle \hat{R}_h^n - \sigma_h^n, \varphi \phi_z \rangle_{\omega_z} \right\}.$$

In view of definitions (2.25) and (2.23) of σ_h^n and s_z^n , we see that

$$\langle \mathcal{G}_h^n, \varphi \phi_z \rangle = \int_{\omega_z} \mu^2 \nabla U_h^n \cdot \nabla(\varphi \phi_z) - (\hat{R}_h^n - \sigma_h^n) \varphi \phi_z = \int_{\omega_z} \mu^2 \nabla U_h^n \cdot \nabla((\varphi - \tilde{\varphi}_z) \phi_z) - \hat{R}_h^n (\varphi - \tilde{\varphi}_z) \phi_z$$

where $\tilde{\varphi}_z$ is the constant

$$\tilde{\varphi}_z := \begin{cases} \frac{\int_{\omega_z} \varphi \phi_z}{\int_{\omega_z} \phi_z}, & \text{if } z \in \mathcal{P}_h \cap \Omega \\ 0, & \text{if } z \in \mathcal{P}_h \cap \partial\Omega. \end{cases} \tag{3.8}$$

We now recall the definitions (2.20) of \hat{R}_h^n and R_h^n , and integrate by parts to infer that

$$\begin{aligned} \langle \mathcal{G}_h^n, \varphi \phi_z \rangle &= \int_{\omega_z} \mu^2 \nabla U_h^n \cdot \nabla((\varphi - \tilde{\varphi}_z) \phi_z) + \nabla(\mu^2) \cdot \nabla U_h^n (\varphi - \tilde{\varphi}_z) \phi_z - R_h^n (\varphi - \tilde{\varphi}_z) \phi_z \\ &= - \int_{\gamma_z} J_h^n (\varphi - \tilde{\varphi}_z) \phi_z - \int_{\omega_z} (R_h^n - \tilde{R}_z^n) (\varphi - \tilde{\varphi}_z) \phi_z, \end{aligned} \tag{3.9}$$

because of the orthogonality relation $\int_{\omega_z} \tilde{R}_z^n (\varphi - \tilde{\varphi}_z) \phi_z = 0$ which, in light of (3.8), holds for arbitrary constants \tilde{R}_z^n for $z \in \mathcal{P}_h \cap \Omega$ and $\tilde{R}_z^n = 0$ for $z \in \mathcal{P}_h \cap \partial\Omega$.

Standard interpolation arguments based on a trace theorem and the Bramble-Hilbert lemma yield [11, 24]

$$|\langle \mathcal{G}_h^n, \varphi \phi_z \rangle| \lesssim \left(h_z^{\frac{1}{2}} \|J_h^n\|_{\gamma_z} + h_z \left\| R_h^n - \tilde{R}_z^n \right\|_{\omega_z} \right) \|\nabla \varphi\|_{\omega_z}.$$

Finally, the asserted estimate (3.5) follows at once upon choosing the optimal value (3.7) for \tilde{R}_z^n , adding over $z \in \mathcal{P}_h \setminus \mathcal{C}_h^n$, and using the finite overlapping property of the stars ω_z . \square

The second step to prove the upper bound is to show that the term $\int_{t_{n-1}}^{t_n} \langle \sigma_h^n - \sigma, U_h - u \rangle dt$ admits a lower bound. The conformity assumption $\mathcal{K}_h^n \subset \mathcal{K}$, never used before, will play an essential role now.

Lemma 3.2 (lower bound of Lagrange multipliers). *Let $\{U_h^n\}_{n=1}^N$ solve the discrete problem (2.6) and let the continuous and discrete Lagrange multipliers σ and σ_h^n be defined in (2.22) and (2.24), respectively. Then the following inequality holds*

$$\int_{t_{n-1}}^{t_n} \langle \sigma_h^n - \sigma, U_h - u \rangle dt \geq - \sum_{z \in \mathcal{C}_h^n \cup \mathcal{F}_h^n} \frac{\tau_n}{2} \langle \sigma_h^n, (U_h^n - U_h^{n-1}) \phi_z \rangle + \sum_{z \in \mathcal{F}_h^n} \tau_n s_z^n d_z^n, \tag{3.10}$$

where the constants s_z^n are defined in (2.23) and

$$d_z^n := \int_{\omega_z} (U_h^n - \chi_h^n) \phi_z = \int_{\omega_z} (U_h^n - \chi_h) \phi_z \geq 0. \tag{3.11}$$

Proof. In view of (2.22) and (2.4), we have $\langle \sigma, u - v \rangle \leq 0$ for all $v \in \mathcal{K}$. Since $U_h(t) \in \mathcal{K}$ a.e. $t \in [0, T]$ according to (3.1), we obtain $\langle \sigma, u - U_h \rangle \geq 0$, whence

$$\langle \sigma_h^n - \sigma, U_h - u \rangle \geq \langle \sigma_h^n, U_h - u \rangle = \sum_{z \in \mathcal{P}_h} \langle \sigma_h^n, (U_h - u) \phi_z \rangle_{\omega_z}.$$

The crucial property $\sigma_h^n \leq 0$, in conjunction with the consequence $u \geq \chi = \chi_h^n$ of (3.1), implies that

$$\langle \sigma_h^n, (U_h - u) \phi_z \rangle = \langle \sigma_h^n, (U_h - \chi_h + \chi_h - u) \phi_z \rangle_{\omega_z} \geq \langle \sigma_h^n, (U_h - \chi_h) \phi_z \rangle_{\omega_z}.$$

Using definition $U_h = l(t)U_h^{n-1} + (1 - l(t))U_h^n$, with $l(t)$ given in (2.17), and integrating in time yields

$$\begin{aligned} \int_{t_{n-1}}^{t_n} \langle \sigma_h^n, (U_h - \chi_h) \phi_z \rangle dt &= \frac{\tau_n}{2} \langle \sigma_h^n, (U_h^{n-1} + U_h^n - 2\chi_h) \phi_z \rangle \\ &= \frac{\tau_n}{2} \langle \sigma_h^n, (U_h^{n-1} - U_h^n) \phi_z \rangle + \tau_n \langle \sigma_h^n, (U_h^n - \chi_h) \phi_z \rangle. \end{aligned}$$

We finally observe that $\langle \sigma_h^n, \varphi \phi_z \rangle = 0$ for $z \in \mathcal{N}_h^n$, because $s_z^n = 0$, and $U_h^n = \chi_h$ in ω_z for $z \in \mathcal{C}_h^n$. Therefore $\langle \sigma_h^n, (U_h^n - \chi_h) \phi_z \rangle = s_z^n d_z^n$ for $z \in \mathcal{F}_h^n$ and zero otherwise, whence the desired estimate (3.10) follows immediately. \square

Replacing the estimates of Lemmata 3.1 and 3.2 into (3.4) yields the main result of this section.

Theorem 3.3 (upper bound: piecewise linear time-independent obstacles). *Let u be the continuous solution of (2.4) and $\{U_h^n\}_{n=1}^N$ be the discrete solution of (2.6). Let data f and u_0 satisfy $f \in L^2(0, T; L^2(\Omega))$ and $u_0 \in L^2(\Omega)$. If σ_h^n denotes the discrete Lagrange multiplier of (2.25), and s_z^n, d_z^n indicate the constants defined in (2.23) and (3.11), then the following a posteriori upper bound holds*

$$\begin{aligned} \|(U_h - u)(T)\|^2 &+ \frac{1}{4} \int_0^T \left(\|\overline{U}_h - u\|^2 + \|U_h - u\|^2 \right) dt + \frac{1}{48\gamma^2} \int_0^T \|\partial_t(U_h - u) + (\overline{\sigma}_h - \sigma)\|_*^2 dt \\ &\leq \|U_h^0 - u_0\|^2 && \text{initial error} \\ &+ \sum_{n=1}^N \frac{4}{3} \gamma^2 \tau_n \|U_h^n - U_h^{n-1}\|^2 && \text{time error} \\ &+ \sum_{n=1}^N \tau_n \left\{ \sum_{z \in \mathcal{P}_h \setminus \mathcal{C}_h^n} \lambda C_G (\eta_z^n)^2 - \sum_{z \in \mathcal{F}_h^n} 2s_z^n d_z^n \right\} && \text{space error} \\ &+ \sum_{n=1}^N \sum_{z \in \mathcal{C}_h^n \cup \mathcal{F}_h^n} \tau_n \langle \sigma_h^n, (U_h^n - U_h^{n-1}) \phi_z \rangle && \text{mixed error} \\ &+ \lambda \int_0^T \|\overline{F}_h - f\|_*^2 dt && \text{data consistency} \end{aligned}$$

with constants γ^2, C_G given in (2.12), (3.5), $\lambda := 8 + \frac{1}{16\gamma^2}$, and space error estimator η_z^n given in (3.6).

Remark 3.4 (oscillation term). The spatial data oscillation term is hidden in the second part $h_z \|R_h^n - \tilde{R}_z^n\|_{\omega_z}$ of η_z^n . In the case of the Poisson equation, we have $R_h^n = F_h^n$ if $z \in \mathcal{P}_h \cap \Omega$, and such a term reduces to the usual data oscillation $h_z \|F_h^n - \tilde{F}_z^n\|_{\omega_z}$. This quantity is generically of higher order than the interior residual $h_z \|F_h^n\|_{\omega_z}$, as can be seen in the numerical experiments of Section 5; see also [11, 20].

Remark 3.5 (localization). The space error indicator η_z^n is fully localized, *i.e.*, there is no contribution from $z \in \mathcal{C}_h^n$, the discrete contact set. Note that this is consistent with the absence of obstacle approximation error because $\chi_h = \chi$. Likewise, the term $-s_z^n d_z^n \geq 0$ contributes only when $z \in \mathcal{F}_h^n$. This extends the localized elliptic estimates of [11, 20] to the parabolic setting. One may also wonder whether the sets of full-contact nodes \mathcal{C}_h^n and free boundary nodes \mathcal{F}_h^n are good approximations of the actual contact region and free boundary, respectively. We will explore this point further *via* numerical experiments in Section 5.

Remark 3.6 (mixed error term). The mixed error estimator mimics the nonlinear term in (2.14), and combines effects of both time and space discretization. For $z \in \mathcal{C}_h^n$, this term contributes solely where $U_h^n \neq U_h^{n-1}$, that is close to the discrete free boundary \mathcal{F}_h^n because $\chi_h(t) \equiv \chi_h$, for $t \in [0, T]$. The numerical results in Section 5 show that this term is relatively small and decays with higher order than other terms of the proposed space and time error estimators.

3.2. Lower bound

We first derive the lower bound of the local error based on our space error indicator η_z^n . Since localization entails $\eta_z^n = 0$ for $z \in \mathcal{C}_h^n$, the contact set, we just have to consider $z \in \mathcal{P}_h \setminus \mathcal{C}_h^n$.

Lemma 3.7 (lower bound for space error). *Under the same assumptions as in Theorem 3.3, we have the following local lower bound*

$$h_z^{1/2} \|J_h^n\|_{\gamma_z} \lesssim \gamma \|U_h^n - u\|_{\omega_z} + \|\partial_t(U_h - u) + (\sigma_h^n - \sigma)\|_{*,\omega_z} + \sum_{x \in (\mathcal{P}_h \setminus \mathcal{C}_h^n) \cap \omega_z} h_x \|R_h^n - \tilde{R}_x^n\|_{\omega_x} + \|F_h^n - f\|_{*,\omega_z} \quad (3.12)$$

for any $z \in \mathcal{P}_h \setminus \mathcal{C}_h^n$ and $n = 1, \dots, N$.

Proof. Let $z \in \mathcal{P}_h \setminus \mathcal{C}_h^n$ and $\varphi \in H_0^1(\omega_z)$. In view of (3.9) we can write

$$\langle \mathcal{G}_h^n, \varphi \rangle = - \sum_{x \in (\mathcal{P}_h \setminus \mathcal{C}_h^n) \cap \omega_z} \left(\int_{\gamma_x} J_h^n(\varphi - \tilde{\varphi}_x) \phi_x + \int_{\omega_x} (R_h^n - \tilde{R}_x^n)(\varphi - \tilde{\varphi}_x) \phi_x \right).$$

At the same time, the definition (2.26) of Galerkin functional together with (2.8) gives

$$\|\mathcal{G}_h^n\|_{*,\omega_z} \leq 2\gamma \|U_h^n - u\|_{\omega_z} + \|\partial_t(U_h - u) + (\sigma_h^n - \sigma)\|_{*,\omega_z} + \|F_h^n - f\|_{*,\omega_z}.$$

We now proceed as Fierro and Veerer [11] to construct an explicit test function φ to plug into $\langle \mathcal{G}_h^n, \varphi \rangle$; see also Verfürth [24]. Let $E \subset \gamma_z$ be a generic edge and let ω_E denote the union of the elements $S \in \mathcal{T}_h$ sharing E . Consider the bubble functions

$$\psi_E := \prod_{x \in \mathcal{P}_h \cap E} \phi_x, \quad \psi_S := \prod_{x \in \mathcal{P}_h \cap S} \phi_x; \quad (3.13)$$

note that $\omega_E := \text{supp}(\psi_E)$. Let ζ be defined by

$$\zeta = \psi_E - \sum_{x \in \mathcal{P}_h \cap S, S \subset \omega_E} \alpha_{S,x} \psi_S \phi_x$$

with coefficients $\alpha_{S,x} \in \mathbb{R}$ given by the linear system

$$\sum_{x \in \mathcal{P}_h \cap S} \alpha_{S,x} \int_S \psi_S \phi_x \phi_y = \int_S \psi_E \phi_y \quad \forall y \in \mathcal{P}_h \cap S.$$

It is easy to see that $\text{supp } \zeta = \omega_E$, and that $\int_{\omega_y} \zeta \phi_y = 0$ for all $y \in \mathcal{P}_h$. Moreover, ζ satisfies

$$\| \nabla \zeta \|_{\omega_E} + h_z^{-1} \| \zeta \|_{\omega_E} \leq h_z^{-1/2} \| \psi_E \|_E,$$

because $\zeta|_E = \psi_E$. We finally set $\varphi := J_h^n|_E \zeta$ and observe that [24], Lemma 3.3, implies

$$\| J_h^n \|_E^2 \lesssim \sum_{x \in \mathcal{P}_h \setminus \mathcal{C}_h^n} \int_E J_h^n J_h^n \psi_E \phi_x = \sum_{x \in \mathcal{P}_h \setminus \mathcal{C}_h^n} \int_E J_h^n \varphi \phi_x,$$

whence

$$\begin{aligned} \| J_h^n \|_E^2 &\lesssim -\langle \mathcal{G}_h^n, \varphi \rangle_{\omega_E} - \sum_{x \in (\mathcal{P}_h \setminus \mathcal{C}_h^n) \cap \omega_E} \int_{\omega_x} (R_h^n - \tilde{R}_x^n)(\varphi - \tilde{\varphi}_x) \phi_x \\ &\lesssim \| \mathcal{G}_h^n \|_{*, \omega_E} \| \varphi \|_{\omega_E} + \sum_{x \in (\mathcal{P}_h \setminus \mathcal{C}_h^n) \cap \omega_E} h_x \| R_h^n - \tilde{R}_x^n \|_{\omega_x} \| \nabla \varphi \|_{\omega_E} \\ &\lesssim \left(\| \mathcal{G}_h^n \|_{*, \omega_E} + \sum_{x \in (\mathcal{P}_h \setminus \mathcal{C}_h^n) \cap \omega_E} h_x \| R_h^n - \tilde{R}_z^n \|_{\omega_x} \right) h_z^{-1/2} \| J_h^n \|_E. \end{aligned}$$

Consequently, we get the desired result. □

Remark 3.8 (local implies global). Since the local lower bound (3.12) contains local negative norms, and negative norms are nonlocal, it is not clear that squaring and adding (3.12) would lead to a global lower bound. This is indeed the case as the following argument shows. Let $\Lambda \in H^{-1}(\Omega)$, and

$$\varphi_z \in H_0^1(\omega_z) : \quad \| \nabla \varphi_z \|_{\omega_z} = \| \Lambda \|_{*, \omega_z}, \quad \| \Lambda \|_{*, \omega_z}^2 = \langle \Lambda, \varphi_z \rangle \quad \forall z \in \mathcal{P}_h.$$

Then $\varphi = \sum_{z \in \mathcal{P}_h} \varphi_z \in H_0^1(\Omega)$ and $\| \nabla \varphi \|_{\Omega}^2 \lesssim \sum_{z \in \mathcal{P}_h} \| \nabla \varphi_z \|_{\omega_z}^2 = \sum_{z \in \mathcal{P}_h} \| \Lambda \|_{*, \omega_z}^2$ because of the finite overlapping property of the stars $\{ \omega_z \}_{z \in \mathcal{P}_h}$. Hence

$$\sum_{z \in \mathcal{P}_h} \| \Lambda \|_{*, \omega_z}^2 = \sum_{z \in \mathcal{P}_h} \langle \Lambda, \varphi_z \rangle = \langle \Lambda, \varphi \rangle \leq \| \Lambda \|_{*, \Omega} \| \nabla \varphi \|_{\Omega} \leq \| \Lambda \|_{*, \Omega} \left(\sum_{z \in \mathcal{P}_h} \| \Lambda \|_{*, \omega_z}^2 \right)^{1/2};$$

compare with [2], Proposition 3.7, for the heat equation. The reversed inequality is in general not valid.

The following lower estimate is rather elementary due to the structure of the energy error in Theorem 3.3, which involves both \bar{U}_h and U_h . This is to be compared with [2], Proposition 3.6, for the heat equation.

Lemma 3.9 (lower bound for time error). *The following local lower bound holds*

$$\sum_{n=1}^N \tau_n \| \| U_h^n - U_h^{n-1} \| \|^2 \leq 6 \int_0^T \left(\| \bar{U}_h - u \| \|^2 + \| U_h - u \| \|^2 \right) dt.$$

Proof. We have $\tau_n \| \| U_h^n - U_h^{n-1} \| \|^2 = 3 \int_{t_{n-1}}^{t_n} \| \bar{U}_h - U_h \| \|^2 dt \leq 6 \int_{t_{n-1}}^{t_n} \left(\| \bar{U}_h - u \| \|^2 + \| U_h - u \| \|^2 \right) dt$ because of definition (2.16) of \bar{U}_h and U_h , and the triangle inequality. □

4. A POSTERIORI ERROR ESTIMATE: GENERAL OBSTACLES

For option pricing problems, we need to consider obstacles which are neither piecewise constant nor time-independent, as in the previous section. Although one can always use the transformation $v = u - \chi$ and solve the parabolic variational inequality for v , this does not avoid dealing with the obstacle χ especially in defining

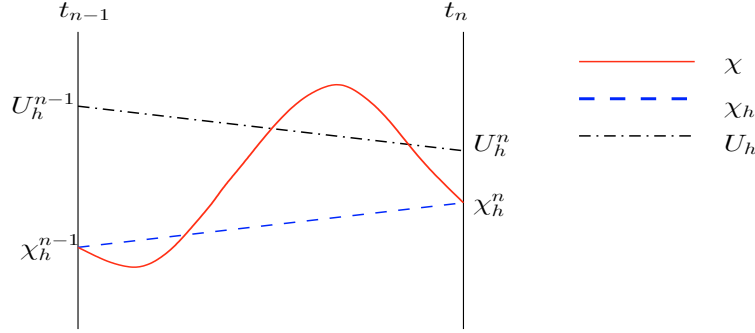


FIGURE 1. Obstacle consistency: If the obstacle χ and its space-time piecewise linear approximation χ_h do not coincide in $\omega_z \times (t_{n-1}, t_n)$ for nodes $z \in \mathcal{P}_h \setminus \mathcal{N}_h^n$, then the quantities $\langle \sigma_h^n, (\chi - U_h)^+ \phi_z \rangle$ and $\langle \sigma_h^n, (\chi_h - \chi)^+ \phi_z \rangle$ measure the local lack of conformity. Note that these quantities vanish for $z \in \mathcal{N}_h^n$, that is for the non-contact nodes.

the contact region. In this section, we consider the case of general obstacles $\chi \in H^1(\mathcal{Q})$ directly. This extension affects only Lemma 3.2, which must be revisited within the present context.

Therefore, in what follows we derive a lower bound for $\int_{t_{n-1}}^{t_n} \langle \sigma_h^n - \sigma, U_h - u \rangle dt$. To this end, we let $\chi_h = l(t)\chi_h^{n-1} + (1 - l(t))\chi_h^n \in C([0, T]; \mathbb{V}_h(\Omega))$ be a space-time piecewise linear approximation of χ , and observe that in general $\chi_h(t) \not\equiv \chi(t)$ for $0 \leq t \leq T$. To handle this lack of consistency, we follow Veerer [23] and introduce the auxiliary function $U_h^* := \max(U_h, \chi) \in \mathcal{K}$. Since $\langle \sigma, u - U_h^* \rangle \geq 0$, we have that

$$\langle \sigma_h^n - \sigma, U_h - u \rangle \geq \langle \sigma_h^n, U_h^* - u \rangle + \langle \sigma - \sigma_h^n, U_h^* - U_h \rangle. \tag{4.1}$$

For the first term on the right-hand-side of (4.1), we invoke $\sigma_h^n \leq 0$ and $\langle \sigma_h^n, (\chi - u)\phi_z \rangle \geq 0$ to obtain

$$\begin{aligned} \langle \sigma_h^n, U_h^* - u \rangle &= \sum_{z \in \mathcal{P}_h} \langle \sigma_h^n, (U_h^* - u)\phi_z \rangle \geq \sum_{z \in \mathcal{P}_h} \langle \sigma_h^n, (U_h^* - \chi)\phi_z \rangle \\ &= \sum_{z \in \mathcal{P}_h} \langle \sigma_h^n, (U_h - \chi_h)\phi_z \rangle + \langle \sigma_h^n, (U_h^* - U_h)\phi_z \rangle + \langle \sigma_h^n, (\chi_h - \chi)\phi_z \rangle. \end{aligned} \tag{4.2}$$

Arguing as in the proof of Lemma 3.2 with the first term on the right-hand side, we deduce

$$\sum_{z \in \mathcal{P}_h} \int_{t_{n-1}}^{t_n} \langle \sigma_h^n, (U_h - \chi_h)\phi_z \rangle dt = - \sum_{z \in \mathcal{P}_h} \frac{\tau_n}{2} \langle \sigma_h^n, ((U_h^n - U_h^{n-1}) - (\chi_h^n - \chi_h^{n-1}))\phi_z \rangle + \sum_{z \in \mathcal{P}_h \setminus \mathcal{C}_h^n} \tau_n s_z^n d_z^n.$$

This step corresponds to that of Lemma 3.2; in fact the first term on the right-hand side is the most general form of the *mixed error* in Theorem 3.3. However, we now have two additional terms in (4.2) that account for the obstacle inconsistent approximation, as illustrated in Figure 1. To bound them we utilize the definition of U_h^* , which results in $U_h^* - U_h = (\chi - U_h)^+$, as well as $\sigma_h^n \leq 0$, and end up with

$$\langle \sigma_h^n, (U_h^* - U_h)\phi_z \rangle \geq \langle \sigma_h^n, (\chi - U_h)^+ \phi_z \rangle, \quad \langle \sigma_h^n, (\chi_h - \chi)\phi_z \rangle \geq \langle \sigma_h^n, (\chi_h - \chi)^+ \phi_z \rangle.$$

We can also rewrite the second term on the right-hand side of (4.1) as follows:

$$\langle \sigma - \sigma_h^n, U_h^* - U_h \rangle = \langle \partial_t(u - U_h) + (\sigma - \sigma_h^n), (\chi - U_h)^+ \rangle - \langle \partial_t(u - U_h), (\chi - U_h)^+ \rangle.$$

The second term on the right-hand side is most problematic. We handle it *via* integration by parts in time:

$$-\int_0^T \langle \partial_t(u - U_h), (\chi - U_h)^+ \rangle = -\langle u - U_h, (\chi - U_h)^+ \rangle \Big|_0^T + \int_0^T \langle u - U_h, \partial_t(\chi - U_h)^+ \rangle dt.$$

Note that we can eliminate the first term on the right-hand side at $t = 0$ because if $\chi_0(x) > U_h^0(x)$ then $u_0(x) \geq \chi_0(x) > U_h^0(x)$ whence $\langle u_0 - U_h^0, (\chi_0 - U_h^0)^+ \rangle \geq 0$.

After applying the Cauchy-Schwarz inequality three times, we arrive at

$$\begin{aligned} \int_0^T \langle \bar{\sigma}_h - \sigma, U_h - u \rangle dt &\geq - \sum_{n=1}^N \left(\sum_{z \in \mathcal{P}_h} \frac{\tau_n}{2} \langle \sigma_h^n, ((U_h^n - U_h^{n-1}) - (\chi_h^n - \chi_h^{n-1})) \phi_z \rangle - \sum_{z \in \mathcal{F}_h^n} \tau_n s_z^n d_z^n \right) \\ &\quad + \sum_{z \in \mathcal{P}_h} \int_0^T \langle \bar{\sigma}_h, ((\chi - U_h)^+ + (\chi_h - \chi)^+) \phi_z \rangle dt \\ &\quad - \frac{\varepsilon_1}{2} \int_0^T \|\partial_t(u - U_h) + (\sigma - \bar{\sigma}_h)\|_*^2 dt - \frac{1}{2\varepsilon_1} \int_0^T \|(\chi - U_h)^+\|^2 dt \\ &\quad - \frac{\varepsilon_2}{2} \|(u - U_h)(T)\|^2 - \frac{1}{2\varepsilon_2} \|(\chi - U_h)^+(T)\|^2 \\ &\quad - \int_0^T \frac{\varepsilon_3}{2} \|u - U_h\|^2 + \frac{1}{2\varepsilon_3} \|\partial_t(\chi - U_h)^+\|_*^2 dt, \end{aligned}$$

with $\varepsilon_1, \varepsilon_2, \varepsilon_3 > 0$ arbitrary. We finally choose $\varepsilon_1 = \frac{1}{96\gamma^2}$, $\varepsilon_2 = \frac{1}{2}$ and $\varepsilon_3 = \frac{1}{8}$, and insert the above estimate into (3.4) to obtain the following upper bound.

Theorem 4.1 (upper bound: general obstacles). *With the same notation as in Theorem 3.3, but general obstacle $\chi \in H^1(Q)$, we have the following upper a posteriori bound*

$$\begin{aligned} &\|(U_h - u)(T)\|^2 + \int_0^T \left(\frac{1}{2} \|\bar{U}_h - u\|^2 + \frac{1}{4} \|U_h - u\|^2 \right) dt + \frac{1}{48\gamma^2} \int_0^T \|\partial_t(U_h - u) + (\bar{\sigma}_h - \sigma)\|_*^2 dt \\ &\leq 2 \|U_h^0 - u_0\|^2 && \text{initial error} \\ &+ \frac{8\gamma^2}{3} \sum_{n=1}^N \tau_n \|U_h^n - U_h^{n-1}\|^2 && \text{time error} \\ &+ 2\lambda C_G \sum_{n=1}^N \sum_{z \in \mathcal{P}_h \setminus \mathcal{C}_h^n} \tau_n (\eta_z^n)^2 - 4 \sum_{n=1}^N \sum_{z \in \mathcal{F}_h^n} \tau_n s_z^n d_z^n && \text{space error} \\ &+ 2 \sum_{n=1}^N \sum_{z \in \mathcal{C}_h^n \cup \mathcal{F}_h^n} \tau_n \langle \sigma_h^n, ((U_h^n - U_h^{n-1}) - (\chi_h^n - \chi_h^{n-1})) \phi_z \rangle && \text{mixed error} \\ &+ 4 \|(\chi - U_h)^+(T)\|^2 + \int_0^T 192 \gamma^2 \|(\chi - U_h)^+\|^2 + 16 \|\partial_t(\chi - U_h)^+\|_*^2 dt && \text{obstacle consistency 1} \\ &- 4 \sum_{n=1}^N \sum_{z \in \mathcal{C}_h^n \cup \mathcal{F}_h^n} \int_{t_{n-1}}^{t_n} \langle \sigma_h^n, \{(\chi - U_h)^+ + (\chi_h - \chi)^+\} \phi_z \rangle dt && \text{obstacle consistency 2} \\ &+ 2\lambda \int_0^T \|\bar{F}_h - f\|_*^2 dt. && \text{data consistency} \end{aligned}$$

Remark 4.2 (obstacle consistency 1). Terms involving $(\chi - U_h)^+$ are only active away from the non-contact set, a crucial localization property, and account for the lack of constraint consistency $U_h < \chi$ in both space and time; see Figure 1.

Remark 4.3 (obstacle consistency 2). The space-time situation $\chi_h > \chi$, depicted in Figure 1, is only detected by the term $\langle \sigma_h^n, (\chi_h - \chi)^+ \phi_z \rangle$. In particular, if $z \in \mathcal{C}_h^n$ is a full-contact node, then this is the only nonzero local indicator. Besides justifying its presence, this argument shows that such a term can be regarded as a complement to the notion of full contact nodes which hinges on the condition $\chi_h^n = \chi^n$ in ω_z ; see Section 2.3. For a kink or cusp pointing downwards the relation $\chi_h > \chi$ is not only to be expected but it might suggest that one needs strong local refinement. This is not true because asymptotically the discrete solution detaches from the obstacle and so $\langle \sigma_h^n, (\chi_h - \chi)^+ \phi_z \rangle = 0$; see [19] for a full discussion.

Remark 4.4 (inactive constraint). For the non-contact nodes \mathcal{N}_h^n , the variational inequality becomes an equality. This is reflected on the vanishing of all terms that account for the unilateral constraint. The resulting estimator reduces to an energy-type estimator for a linear diffusion equation. It is however different from earlier versions [2, 21, 25] in that we develop star-based error indicators, the interior residual is of higher order, and the linear sectorial operator \mathcal{L} is more general than the Laplacian.

Remark 4.5 (lower bounds). The lower bounds proved in Lemmas 3.7 and 3.9 are still valid in this context. The additional terms accounting for non-conformity can all be justified, as explained in Remarks 4.2 and 4.3, except for $\|\partial_t(\chi - U_h)^+\|_*$.

5. NUMERICAL EXPERIMENTS

In this section we present several numerical examples computed with the adaptive finite element toolbox ALBERTA of Schmidt and Siebert [22]. The experiments are meant to demonstrate the localization property, as well as to check the asymptotic convergence rates, of the proposed error estimators with respect to both time and space discretization. We thus consider mostly uniform partitions in time and space, the latter made of triangular elements. We do not attempt here to use our estimators to drive an adaptive algorithm, which is the subject of current research. We provide instead computational evidence that our estimators possess essential information for adaptivity.

5.1. Implementation

In all our numerical experiments, obstacles χ are piecewise smooth functions. We take χ_h and U_h^0 to be piecewise linear interpolants of χ and u_0 , respectively, whereas F_h^n is an approximate L^2 projection of $f(\cdot, t_n)$ into the space of piecewise linears. We note that the free boundary is generally unknown, and so free boundary points are not mesh nodes usually.

In each time step, we use the projective SOR method (PSOR) [9, 12] to solve the resulting finite dimensional linear complementary problem (2.7). The termination condition for the PSOR method is to make the relative residual less than 10^{-8} .

We denote by \mathcal{E} the total error estimator

$$\mathcal{E} := (\mathcal{E}_h^2 + \mathcal{E}_\tau^2 + \mathcal{E}_{\tau h}^2 + \mathcal{E}_\chi^2)^{\frac{1}{2}},$$

where \mathcal{E}_h , \mathcal{E}_τ , $\mathcal{E}_{\tau h}$, and \mathcal{E}_χ are the space, time, mixed, and obstacle consistency error estimators

$$\begin{aligned} \mathcal{E}_h &:= (\mathcal{E}_{h,1}^2 + \mathcal{E}_{h,2}^2 + \mathcal{E}_{h,3}^2)^{\frac{1}{2}} \\ \mathcal{E}_\tau &:= \left(\sum_{n=1}^N \tau_n \|U_h^n - U_h^{n-1}\|^2 \right)^{\frac{1}{2}} \end{aligned}$$

$$\begin{aligned} \mathcal{E}_{\tau h} &:= \left(\sum_{n=1}^N \tau_n \sum_{z \in \mathcal{C}_h^n \cup \mathcal{F}_h^n} \langle \sigma_h^n, ((U_h^n - U_h^{n-1}) - (\chi_h^n - \chi_h^{n-1})) \phi_z \rangle \right)^{\frac{1}{2}} \\ \mathcal{E}_\chi &:= \left(\int_0^T \|\chi - U_h\|^2 dt - \sum_{n=1}^N \sum_{z \in \mathcal{C}_h^n \cup \mathcal{F}_h^n} \int_{t_{n-1}}^{t_n} \langle \sigma_h^n, \{(\chi - U_h)^+ + (\chi_h - \chi)^+\} \phi_z \rangle dt \right)^{\frac{1}{2}}, \end{aligned}$$

with $\mathcal{E}_{h,i} := (\sum_{n=1}^N \tau_n E_{h,i}^n)^{1/2}$ for $i = 1, 2, 3$, and

$$E_{h,1}^n := \sum_{z \in \mathcal{P}_h \setminus \mathcal{C}_h^n} h_z \|J_h^n\|_{\gamma_z}^2 \quad E_{h,2}^n := \sum_{z \in \mathcal{P}_h \setminus \mathcal{C}_h^n} h_z^2 \left\| R_h^n - \tilde{R}_z^n \right\|_{\omega_z}^2 \quad E_{h,3}^n := - \sum_{z \in \mathcal{F}_h^n} s_z^n d_z^n.$$

In the experiments below we examine the relative sizes of these four quantities. We also take all constants in the proposed error estimators to be 1; hence no ad-hoc scaling is used. We employ the notation:

e = energy error $\|u - U\|_{L^2(0,T;H^1(\Omega))}$

EOC = experimental order of convergence (based on last two experiments)

N = number of time steps

DOF = number of degrees of freedom in space.

Remark 5.1 (nonhomogeneous Dirichlet conditions). Since $u = g \neq 0$ on $\Gamma = \partial\Omega \times (0, T)$ in our experiments, we take $U(z) = g(z)$ at boundary nodes $z \in \mathcal{P}_h \cap \partial\Omega$. For $d = 1$ and $d = 2$ with piecewise linear g , this is equivalent to the problem with zero boundary data. Otherwise, in addition to the above estimators, there is an interpolation error which is neglected because its order is higher than $\mathcal{O}(h)$ for smooth g .

Remark 5.2 (negative norm estimators). We implement all the estimators in Theorem 4.1, except for $\|\partial_t(\chi - U_h)^+\|_*$ and $\|\bar{F}_h - f\|_*$. We would expect the first one to be of at least the same order as $\|(\chi - U_h)^+\|$ (see example 5.5 for numerical evidence) and the second term to be of higher order than $\mathcal{O}(h)$. In fact, since f is always Lipschitz continuous across the free boundary and smooth elsewhere, we expect its L^2 -projection \bar{F}_h with (7th order) quadrature into the space of piecewise linears to superconverge in $H^{-1}(\Omega)$.

Remark 5.3 (nodal-based space error indicator). The space error estimator \mathcal{E}_h can be written as $\mathcal{E}_h = \sum_{n=1}^N \sum_{z \in \mathcal{P}_h} \tau_n \mathfrak{E}_z^n$, where the nodal-based space error indicator \mathfrak{E}_z^n is given by

$$\mathfrak{E}_z^n := \begin{cases} \left(h_z \|J_h^n\|_{\gamma_z}^2 + h_z^2 \left\| R_h^n - \tilde{R}_z^n \right\|_{\omega_z}^2 - s_z^n d_z^n \right)^{\frac{1}{2}} & z \in \mathcal{F}_h^n \\ \left(h_z \|J_h^n\|_{\gamma_z}^2 + h_z^2 \left\| R_h^n - \tilde{R}_z^n \right\|_{\omega_z}^2 \right)^{\frac{1}{2}} & z \in \mathcal{N}_h^n \\ 0 & z \in \mathcal{C}_h^n. \end{cases}$$

We see that \mathfrak{E}_z^n vanishes at full-contact nodes $z \in \mathcal{C}_h^n$, the crucial localization property alluded to in Remark 3.5. On the other hand, this estimator disregards the case $\chi_h \neq \chi$, which is taken care of by the obstacle consistency estimator \mathcal{E}_χ .

5.2. 1d tent obstacle: case $\chi_h = \chi$

We take $\mathcal{L} := -\frac{\partial^2}{\partial x^2}$, the domain $\Omega := [-1.0, 1.0]$, the time interval $[0.5, 1.0]$, and the noncontact and contact sets to be $\mathcal{N} := \{|x| > t/6\}$ and $\mathcal{C} := \{|x| \leq t/6\}$. If the obstacle is $\chi(x) = 1 - 3|x|$, then the exact solution u

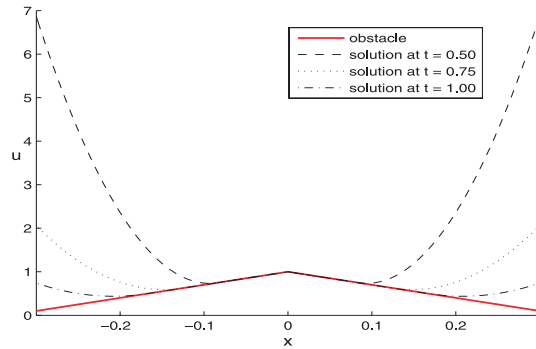


FIGURE 2. 1d tent obstacle: Exact solution $u(\cdot, t)$ at times $t = 0.5, 0.75, 1.0$. The obstacle χ is piecewise linear with a kink at $x = 0$, belonging to all partitions. This implies $\chi_h = \chi$.

TABLE 1. 1d tent obstacle problem ($\chi_h = \chi$): The space and time estimators $\mathcal{E}_h, \mathcal{E}_\tau$, decrease with optimal order 1, but the mixed estimator $\mathcal{E}_{\tau h}$ is of higher order. The ratio between total estimator \mathcal{E} and energy error e is quite stable and of moderate size.

N	DOF	\mathcal{E}_h	\mathcal{E}_τ	$\mathcal{E}_{\tau h}$	\mathcal{E}	e	\mathcal{E}/e
64	127	2.256e+0	2.121e+0	2.731e-2	3.097e+0	7.347e-1	4.219
128	255	1.138e+0	1.059e+0	9.686e-3	1.555e+0	3.700e-1	4.202
256	511	5.716e-1	5.294e-1	3.338e-3	7.791e-1	1.857e-1	4.202
512	1023	2.864e-1	2.646e-1	1.181e-3	3.900e-1	9.301e-2	4.184
1024	2047	1.434e-1	1.323e-1	4.148e-4	1.951e-1	4.655e-2	4.184
EOC		0.998	1.000	1.510	0.999	0.999	–

and forcing function f are given by

$$u(x, t) = \begin{cases} 36t^{-2}x^2 - (3 + 12t^{-1})|x| + 2 & \text{in } \mathcal{N} \\ 1 - 3|x| & \text{in } \mathcal{C}, \end{cases}$$

$$f(x, t) = \begin{cases} -12t^{-2}(6t^{-1}x^2 - |x| + 6) & \text{in } \mathcal{N} \\ -72t^{-2} & \text{in } \mathcal{C}. \end{cases}$$

Function u is depicted in Figure 2 at times $t = 0.5, 0.75$, and 1.0 .

To test the asymptotic convergence rates of both the proposed error estimator \mathcal{E} and exact error e , we halve time step τ and space meshsize h in each experiment and report the results in Table 1 and Figure 3. To investigate the decay of each component $\mathcal{E}_{h,i}$ of the space estimator \mathcal{E}_h we fix the time-step to be $\tau = 2.5 \times 10^{-4}$, so small that the error is dominated by the space discretization. Table 2 displays their behavior under uniform space refinement: the nodal-based estimator $\mathcal{E}_{h,1}$ exhibits optimal order 1 and dominates the other two terms.

We display in Figure 4 the nodal-based space error estimator \mathfrak{E}_z^n at different stages $t_n = 0.6, 0.8, 1.0$ of the evolution. We see that \mathfrak{E}_z^n vanishes at full-contact nodes $z \in \mathcal{C}_h^n$, as predicted by theory, and that the exact free-boundary is captured within one element. This is further documented in Table 3 which shows exact and approximate free boundary locations at times $t_n = 0.6, 0.8, 1.0$.

5.3. 1d tent obstacle: case $\chi_h \neq \chi$

In general, we cannot expect the underlying mesh to match the singular behavior of the obstacle, as in Example 5.2, even for piecewise linear obstacles. This happens, for instance, when the obstacles change in time. The question thus arises whether or not the proposed error estimator \mathcal{E} is able to capture the correct behavior of the solution when a singularity is not resolved by the mesh.

TABLE 2. Decay of each component $\mathcal{E}_{h,i}$ of the space estimator \mathcal{E}_h for a fixed time-step $\tau = 2.5 \times 10^{-4}$ so small that the time estimator \mathcal{E}_τ is insignificant. Left: 1d tent obstacle problem; Right: 2d oscillating moving obstacle problem. In both cases the nodal-based estimator $\mathcal{E}_{h,1}$ exhibits the expected order 1 whereas the other two superconverge.

1d tent obstacle example ($\chi_h = \chi$)				2d oscillating moving circle example			
DOF	$\mathcal{E}_{h,1}$	$\mathcal{E}_{h,2}$	$\mathcal{E}_{h,3}$	DOF	$\mathcal{E}_{h,1}$	$\mathcal{E}_{h,2}$	$\mathcal{E}_{h,3}$
129	2.282	3.034e-1	4.929e-2	145	1.094	1.323	1.194e-2
257	1.144	1.073e-1	1.823e-2	545	5.660e-1	4.974e-1	3.936e-3
513	5.729e-1	3.792e-2	6.295e-3	2113	2.880e-1	1.817e-1	1.368e-3
1025	2.866e-1	1.341e-2	2.250e-3	8321	1.453e-1	6.532e-2	4.652e-4
2049	1.434e-1	4.740e-3	7.903e-4	33 025	7.295e-2	2.329e-2	1.617e-4
EOC	0.999	1.500	1.509	EOC	0.994	1.488	1.525

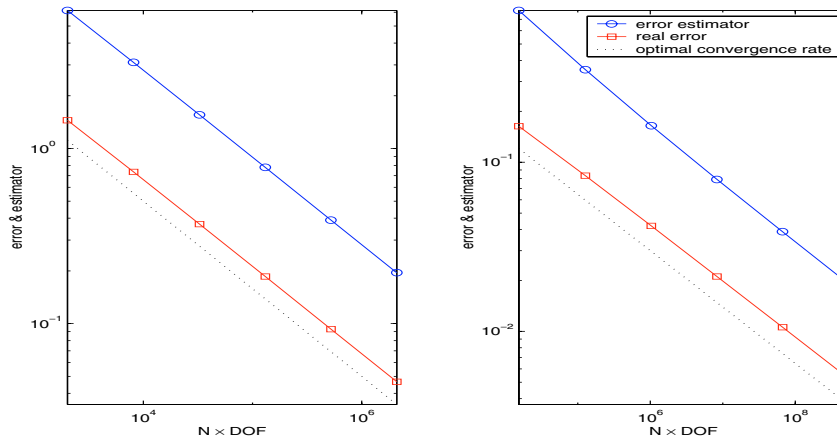


FIGURE 3. Error estimator \mathcal{E} and energy error e vs. total number of degrees of freedom ($N \cdot \text{DOF}$) for 1d tent obstacle example with $\chi_h = \chi$ (left) and 2d oscillating moving circle problem (right). Since $N \cdot \text{DOF} \simeq \frac{1}{\tau h^d} \simeq \frac{1}{h^{d+1}}$, provided $\tau \simeq h$, the optimal error decay is $\mathcal{O}(h) = \mathcal{O}((N \cdot \text{DOF})^{-\frac{1}{d+1}})$ and is indicated by the dotted lines with slopes $-1/2$ (left) for $d = 1$ and $-1/3$ (right) for $d = 2$. This shows optimal decay of both \mathcal{E} and e .

TABLE 3. 1d tent obstacle problem ($\chi_h = \chi$): Since the meshsize is $h \approx 7.8 \times 10^{-3}$ the FEM captures the exact free boundary within one element.

Time	Exact free boundary	Approx free boundary
0.6	$\pm 1.0000 \times 10^{-1}$	$\pm 1.0156 \times 10^{-1}$
0.8	$\pm 1.3333 \times 10^{-1}$	$\pm 1.3328 \times 10^{-1}$
1.0	$\pm 1.6667 \times 10^{-1}$	$\pm 1.6406 \times 10^{-1}$

To answer this question, we modify Example 5.2 by the shift $v(x - \frac{1}{3}, t)$ for $v = u, \chi, f$ but keep the same meshes and time steps as before. In this case, the kink at $x = 1/3$ is never a mesh point and $\chi_h \neq \chi$. Since χ is almost in $H^{3/2}$ we expect a rate of convergence 0.5 in H^1 . This is confirmed by the results of Table 4, which also shows that the only estimator that detects this reduced order is \mathcal{E}_χ , the obstacle consistency error estimator. We observe that \mathcal{E}_h and \mathcal{E}_τ dominate at the beginning and it takes quite awhile to reach the asymptotic regime.

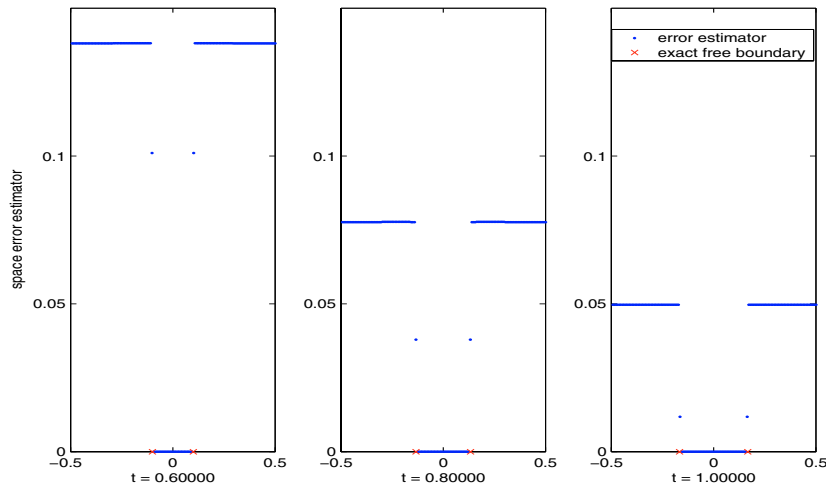


FIGURE 4. 1d tent obstacle example: Nodal-based space error estimator \mathfrak{E}_z^n at times $t_n = 0.6, 0.8, 1.0$ for $\text{DOF} = 255$ and $\tau = 2.5 \times 10^{-4}$. The localization property that \mathfrak{E}_z^n vanishes at the full-contact nodes $z \in \mathcal{C}_h^n$ is clearly visible, along with the fact that free-boundary approximation takes place within one element (see Tab. 3).

TABLE 4. 1d tent obstacle problem ($\chi_h \neq \chi$): The kink is not resolved by the underlying meshes with uniform mesh refinement. The only estimator that detects the reduced order 0.5 is \mathcal{E}_χ . The total estimator is dominated by \mathcal{E}_h and \mathcal{E}_τ at the beginning but eventually \mathcal{E}_χ takes over. This combined effect is reflected in the behavior of the total estimator \mathcal{E} .

N	DOF	\mathcal{E}_h	\mathcal{E}_τ	$\mathcal{E}_{\tau h}$	\mathcal{E}_χ	\mathcal{E}	e	\mathcal{E}/e
1024	2047	1.434e-1	1.548e-1	4.154e-4	9.882e-2	2.330e-1	8.175e-2	2.850
2048	4095	7.172e-2	7.741e-2	1.466e-4	6.988e-2	1.266e-1	5.050e-2	2.507
4096	8191	3.587e-2	3.871e-2	5.181e-5	4.941e-2	7.229e-2	3.282e-2	2.203
8192	16383	1.794e-2	1.935e-2	1.831e-5	3.494e-2	4.378e-2	2.213e-2	1.978
16384	32767	8.970e-3	9.676e-3	6.471e-6	2.471e-2	2.801e-2	1.527e-2	1.834
EOC		1.000	1.000	1.501	0.500	0.644	0.535	-

We wonder whether making a suitable local mesh refinement near the kink may restore the optimal linear rate. We conduct an experiment consisting of locally refined meshes only at the kink location, where the meshsize is h^2 , whereas it remains uniform and equal to h elsewhere. The interpolation error in H^1 becomes now proportional to h , both at the kink location and elsewhere, because the error in W_∞^1 is $\mathcal{O}(1)$ and $\mathcal{O}(h)$, respectively. This heuristic argument is corroborated by the results of Table 5, which illustrates the potentials of mesh refinement to achieve optimal complexity along with the importance of \mathcal{E}_χ .

5.4. 1d American option

In American option pricing problems, we start from an initial condition u_0 , as in (1.3), which is in the Sobolev space $H^{\frac{3}{2}-\epsilon}$ for any $\epsilon > 0$ but not in any smoother regularity class. The *a priori* error estimates of [18] imply a rate of convergence $\mathcal{O}(\tau^{1/2})$ for $u_0 \in H^1$ and $\mathcal{O}(\tau)$ for $u_0 \in H^2$. Given the fractional regularity right in the middle between H^1 and H^2 , we expect, from interpolation theory, that the convergence rate with uniform time-step would be about $\mathcal{O}(\tau^{3/4})$. Our experiments confirm this expectation.

TABLE 5. 1d tent obstacle problem ($\chi_h \neq \chi$): The underlying partition is locally refined at the kink location, where the meshsize is h^2 , but is otherwise uniform with meshsize h . This restores the optimal linear rate for both \mathcal{E}_χ and e , as well as the total estimator \mathcal{E} (compared with the reduced rate reported in Tab. 4 for uniform meshes).

N	DOF	\mathcal{E}_h	\mathcal{E}_τ	$\mathcal{E}_{\tau h}$	\mathcal{E}_χ	\mathcal{E}	e	\mathcal{E}/e
32	45	8.710	4.915	1.787e-1	1.398e-1	1.000e+1	2.802	3.570
64	93	4.477	2.467	5.648e-2	9.882e-2	5.113	1.431	3.573
128	191	2.267	1.236	1.947e-2	3.494e-2	2.583	7.230e-1	3.572
256	382	1.141	6.186e-1	6.631e-3	1.747e-2	1.298	3.634e-1	3.572
512	767	5.723e-1	3.095e-1	2.326e-3	8.735e-3	6.507e-1	1.822e-1	3.572
EOC		0.995	0.999	1.511	1.000	0.996	0.996	-

TABLE 6. 1d American put option problem: Uniform time and space partitions yield suboptimal rates for \mathcal{E}_τ and \mathcal{E}_χ due to the fractional regularity of the initial condition, which is about $H^{3/2}$. This explains the order of about 0.75 of \mathcal{E}_τ , that accounts for the initial transient regime, but not quite the suboptimal order of \mathcal{E}_χ .

N	DOF	\mathcal{E}_h	\mathcal{E}_τ	$\mathcal{E}_{\tau h}$	\mathcal{E}_χ	\mathcal{E}
128	511	4.353e-2	1.149e-1	3.240e-3	3.843e-1	4.035e-1
256	1023	2.172e-2	7.023e-2	1.147e-3	2.434e-1	2.543e-1
512	2047	1.091e-2	5.026e-2	4.035e-4	1.195e-1	1.301e-1
1024	4095	5.461e-3	2.940e-2	1.416e-4	7.581e-2	8.150e-2
2048	8191	2.736e-3	1.751e-2	4.980e-5	4.931e-2	5.240e-2
EOC		0.997	0.748	1.505	0.620	0.637

We take an American put option problem on a single stock with strike price $K = 100$, maturity time $T = 0.5$ year, volatility $\alpha = 0.4$, interest rate $r = 6\%$, and forcing $f = 0$. We choose the space domain to be $\Omega = (-1, 7)$. Table 6 displays all four estimators and \mathcal{E}_τ has indeed the expected rate of about 0.75.

We now explore the effect of refining the time partition to restore the optimal convergence rate. We design an algebraically graded time grid

$$t_n = \left(\frac{n}{N}\right)^\beta \quad \forall 1 \leq n \leq N,$$

with $\beta > 0$ to be determined so that the time error estimator $\mathcal{E}_\tau \approx \mathcal{O}(N^{-1})$. The time-step τ_n reads

$$\tau_n = \left(\frac{n}{N}\right)^\beta - \left(\frac{n-1}{N}\right)^\beta \approx \frac{\beta}{N} \left(\frac{n}{N}\right)^{\beta-1} \quad \Rightarrow \quad \tau_n \approx \frac{\beta}{N} t_n^{1-1/\beta}.$$

We recall the regularizing effect for linear parabolic problems, namely,

$$\|\partial_t u(\cdot, t)\|_{H^1} \approx \|u(\cdot, t)\|_{H^3} \lesssim t^{-3/4}$$

provided the initial condition $u_0 \in H^{3/2}$. We proceed heuristically and assume the same asymptotic behavior to be valid for parabolic variational inequalities. We next formally replace $\|U_h^n - U_h^{n-1}\| \lesssim \int_{t_{n-1}}^{t_n} \|\partial_t u(\cdot, t)\| dt$ in the definition of \mathcal{E}_τ to get

$$\mathcal{E}_\tau^2 \approx \sum_{n=1}^N \int_{t_{n-1}}^{t_n} \|\partial_t u(\cdot, t)\|^2 \tau_n^2 dt \approx \frac{\beta}{N} \int_0^T t^{-3/2+2(1-1/\beta)} dt \approx \mathcal{O}(N^{-1}),$$

provided $\beta > 4/3$. This argument can be made rigorous for linear parabolic equations upon using Theorem 4.5 of [26] and carefully approximating the solution on the first time interval. To test this heuristic argument for

TABLE 7. 1d American put option problem: Algebraically graded time partition $t_n = (\frac{n}{N})^{3/2}$ and uniform space mesh. This grading restores the optimal linear convergence rate of both \mathcal{E}_τ and \mathcal{E}_χ (compared with Tab. 6).

N	DOF	\mathcal{E}_h	\mathcal{E}_τ	$\mathcal{E}_{\tau h}$	\mathcal{E}_χ	\mathcal{E}
80	1023	2.386e-2	8.152e-2	1.945e-3	1.833e-1	2.021e-1
160	2047	1.159e-2	4.397e-2	6.693e-4	8.679e-2	9.798e-2
320	4095	5.657e-3	2.235e-2	2.313e-4	4.385e-2	4.954e-2
640	8191	2.793e-3	1.137e-2	8.030e-5	2.238e-2	2.526e-2
1280	16383	1.388e-3	5.899e-3	2.787e-5	1.162e-2	1.310e-2
EOC		1.018	0.975	1.526	0.970	0.972

parabolic variational inequalities, we take $\beta = 1.5$ and report the results in Table 7. We see that this properly chosen time partition restores the optimal convergence rate not only for \mathcal{E}_τ but also for \mathcal{E}_χ . Moreover, this argument explains why uniform time stepping, *i.e.* $\beta = 1$, yields a suboptimal convergence rate for the time estimator \mathcal{E}_τ (see Tab. 6).

5.5. 1d American option with moving obstacle

To test the asymptotic behavior of the obstacle consistency term $\|\partial_t(\chi - U_h)^+\|_*$, which we omitted in \mathcal{E} , we modify the previous American option problem in the following way: from time $t = 0$ to 0.5, we still have the same American option pricing problem as in Section 5.4. From time $t = 0.5$ to 1.0, we raise the obstacle at a constant rate $\xi \in \mathbb{R}_+$. In other words, the obstacle in the previous example has been replaced by:

$$\chi(x, t) := (K - e^x)^+ [1 + \xi(t - 0.5)^+] \quad x \in (-1, 7), t \in [0, T].$$

In this way, we exclude the initial transient region from our consideration and the singular point $\log(K)$ is always a mesh point. Also we choose the speed ξ moderate to prevent the free boundary point to recede to $\log(K)$. Similar to the analysis for the last example, the uniform space mesh and algebraically graded time partition should give optimal convergence rate as before. We report in Table 8 the mixed error estimator terms $\mathcal{E}_{\tau h}$, \mathcal{E}_χ and

$$\mathcal{E}_\chi^o := \left(\int_0^T \|\partial_t(\chi - U_h)^+\|_{L^2(\Omega)}^2 dt \right)^{\frac{1}{2}}.$$

Since it is difficult to compute the dual norm in the term

$$\mathcal{E}_\chi^* := \left(\int_0^T \|\|\partial_t(\chi - U_h)^+\|\|_*^2 dt \right)^{\frac{1}{2}},$$

we compute the term \mathcal{E}_χ^o with the L^2 -norm instead.

From Table 8 we see that the experimental convergence rate of \mathcal{E}_χ^o is 1.0. Since $\mathcal{E}_\chi^* \lesssim \mathcal{E}_\chi^o$, the numerical results show evidence that \mathcal{E}_χ^* is of at least the same order as the obstacle consistency term \mathcal{E}_χ and this justifies the comments in Remark 5.2. On the other hand, we see that the convergence rate of the mixed error term $\mathcal{E}_{\tau h}$ is greater than 1.0 and becomes closer to 1.0 as the obstacle moves faster and faster. Notice that we omit in Table 8 the space and time error estimators \mathcal{E}_h and \mathcal{E}_τ which also converge at the optimal rate 1.0.

TABLE 8. Modified American put option problem: Algebraically graded time partition $t_n = (\frac{n}{N})^{3/2}$ and uniform space mesh.

ξ		0.01			0.1			1.0		
N	DOF	$\mathcal{E}_{\tau h}$	\mathcal{E}_χ	\mathcal{E}_χ^o	$\mathcal{E}_{\tau h}$	\mathcal{E}_χ	\mathcal{E}_χ^o	$\mathcal{E}_{\tau h}$	\mathcal{E}_χ	\mathcal{E}_χ^o
40	511	1.024e-2	3.116e-1	1.250e-1	1.128e-2	3.321e-1	1.250e-1	8.120e-2	5.144e-1	1.280e-1
80	1023	3.623e-3	1.559e-1	6.311e-2	4.015e-3	1.660e-1	6.310e-2	3.613e-3	2.565e-1	6.421e-2
160	2047	1.255e-3	7.801e-2	3.157e-2	1.523e-3	8.304e-2	3.157e-2	1.895e-3	1.280e-1	3.231e-2
320	4095	4.472e-4	3.902e-2	1.584e-2	5.554e-4	4.153e-2	1.584e-2	8.698e-3	6.398e-2	1.611e-2
EOC		1.489	0.999	0.995	1.455	1.000	0.995	1.123	1.000	1.005

TABLE 9. 2d oscillating moving circle problem: The space and time estimators $\mathcal{E}_h, \mathcal{E}_\tau$, decrease with optimal order 1, but the mixed estimator $\mathcal{E}_{\tau h}$ is of higher order. The ratio between total estimator \mathcal{E} and energy error e is quite stable and of moderate size.

N	DOF	\mathcal{E}_h	\mathcal{E}_τ	$\mathcal{E}_{\tau h}$	\mathcal{E}	e	\mathcal{E}/e
64	1985	3.432e-1	8.110e-2	2.219e-3	3.527e-1	8.328e-2	4.237
128	8065	1.597e-1	4.008e-2	8.087e-4	1.646e-1	4.204e-2	3.922
256	32 513	7.664e-2	1.996e-2	2.899e-4	7.920e-1	2.111e-2	3.745
512	130 561	3.749e-2	9.965e-3	1.037e-4	3.879e-2	1.058e-2	3.663
1024	523 265	1.853e-2	4.980e-3	3.691e-5	1.919e-2	5.297e-3	3.623
EOC		1.017	1.001	1.490	1.015	0.998	-

5.6. 2d oscillating moving circle

Let the operator be $\mathcal{L} := -\Delta$, the domain be $\Omega = [-1, 1]^2$, the time interval be $[0, 0.25]$, and the noncontact and contact sets be $\mathcal{N} := \{|x - c(t)|_2 > r_0(t)\}$ and $\mathcal{C} := \{|x - c(t)|_2 \leq r_0(t)\}$ with

$$r_0(t) = 1/3 + 0.3 \sin(4 \omega \pi t), \quad c(t) = r_1 (\cos(\omega \pi t), \sin(\omega \pi t))^T,$$

and $r_1 = 1/3, \omega = 4.0$. The obstacle is $\chi \equiv 0$, and the exact solution u and forcing function f are

$$u(x, t) = \begin{cases} \frac{1}{2} (|x - c(t)|_2^2 - r_0(t)^2)^2 & \text{in } \mathcal{N} \\ 0 & \text{in } \mathcal{C}, \end{cases}$$

$$f(x, t) = \begin{cases} 4 (r_0^2(t) - 2|x - c(t)|_2^2 - \frac{1}{2} (|x - c(t)|_2^2 - r_0^2(t)) ((x - c(t)) \cdot c'(t) + r_0(t)r_0'(t))) & \text{in } \mathcal{N} \\ -4r_0^2(t) (1 - |x - c(t)|_2^2 + r_0^2(t)) & \text{in } \mathcal{C}. \end{cases}$$

The free boundary is an oscillating circle with radius $r_0(t)$ and center $c(t)$ moving counterclockwise along the circle of radius r_1 centered at the origin. The initial and boundary conditions are given by u .

We halve both time-step τ and space meshsize h in each experiment and report the results in Table 9 and Figure 3; we observe optimal linear convergence rate. We also investigate in Table 2 the decay of the space estimators alone. We fix the time-step $\tau = 2.5 \times 10^{-4}$ and halve the meshsize size in each experiment. We observe optimal linear decay of $\mathcal{E}_{h,1}$ but higher order of convergence for $\mathcal{E}_{h,2}, \mathcal{E}_{h,3}$.

In Figure 5, we show the nodal-based space error indicator \mathfrak{E}_z^n on the cross section $x_2 = 0$ at different stages of the evolution $t_n = 0.02, 0.05, 0.18$. For the same times and cross section, we also compare the exact and approximate free boundaries in Table 10. Their difference is well within one meshsize.

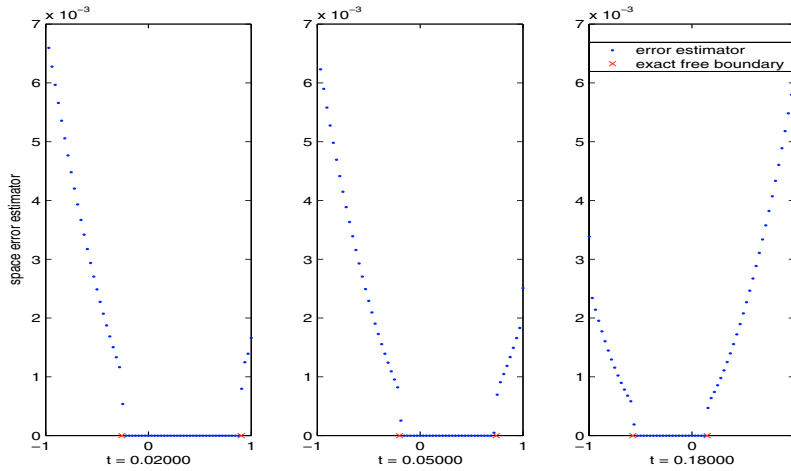


FIGURE 5. 2d oscillating moving circle problem: nodal-based error estimator \mathfrak{E}_z^n in the cross section $x_2 = 0$ for $\text{DOF} = 8065$, $\tau = 2.5 \times 10^{-4}$ and $t_n = 0.02, 0.05, 0.18$. Note the vanishing of \mathfrak{E}_z^n for full-contact nodes and the monotone behavior for the rest.

TABLE 10. 2d oscillating moving circle: Exact and approximate free boundaries on the cross section $x_2 = 0$. Their differences are less than one meshsize, which is about 2.2×10^{-2} .

Time	Exact free boundaries	Approx. free boundaries
0.02	$\{-2.5788 \times 10^{-1}, 9.0361 \times 10^{-1}\}$	$\{-2.5000 \times 10^{-1}, 9.0625 \times 10^{-1}\}$
0.05	$\{-2.0083 \times 10^{-1}, 7.4017 \times 10^{-1}\}$	$\{-1.8750 \times 10^{-1}, 7.1875 \times 10^{-1}\}$
0.18	$\{-5.7430 \times 10^{-1}, 1.4942 \times 10^{-1}\}$	$\{-5.6250 \times 10^{-1}, 1.5625 \times 10^{-1}\}$

6. CONCLUSIONS

We have developed a novel *a posteriori* error analysis for parabolic variational inequalities, including localization features to the non-contact region, and illustrated it with several numerical experiments, some relevant in finance. Upon comparing theory and practice we have the following concluding remarks:

- **Error decay:** For problems with smooth data, the energy error in $L^2(0, T; H^1(\Omega))$ decays linearly, namely $\mathcal{O}(h + \tau)$. Although the experimental evidence is consistent, there seems to be no theoretical justification yet. If the obstacle χ exhibits a singularity not resolved by the mesh, as in Section 5.3, or the initial condition is rough, as in Section 5.4, the actual error decays with a suboptimal rate. Suitable mesh refinement in either space or time appears to cure this problem; see again Sections 5.3 and 5.4.
- **Estimator decay:** The numerical experiments corroborate that the proposed fully localized error estimator \mathcal{E} decays with the same rate as the actual error e . We have demonstrated experimentally that the components $\mathcal{E}_h, \mathcal{E}_\tau, \mathcal{E}_\chi$ of \mathcal{E} provided valuable *a posteriori* information of the solution. We are confident that they can be utilized to drive an adaptive algorithm for problems with unilateral constraints. This is a topic of future research [16].
- **Dominant estimators:** The dominant parts of the error estimator \mathcal{E} for smooth data are $\mathcal{E}_{h,1}$ and \mathcal{E}_τ , which are of order $\mathcal{O}(h)$ and $\mathcal{O}(\tau)$, respectively. Our lower bounds of Section 3.2 are in fact derived for these two terms. The other terms $\mathcal{E}_{h,2}, \mathcal{E}_{h,3}, \mathcal{E}_{\tau h}$ are of higher order in all our test examples. The obstacle consistency term \mathcal{E}_χ is relevant when $\chi_h \neq \chi$, in which case it may be dominant, and Tables 4, 6 and 7 show that it provides correct information for obstacle approximation.
- **Localization of space estimator:** Figures 4 and 5 show that the nodal-based space estimator \mathfrak{E}_z^n vanishes at full-contact nodes $z \in \mathcal{C}_h^n$. Its contribution comes only from the non-contact region where the solution

behaves like the solution of a linear parabolic equation. This estimator yields an upper bound also for globally linear parabolic problems and seems to be new in the literature of parabolic PDE.

- **Exercise boundary approximation:** accurate approximation of the free (exercise) boundary is an important problem in option pricing. Numerical results in Sections 5.2 and 5.6, particularly Figures 4 and 5 as well as Tables 3 and 10, suggest an excellent agreement between approximate and exact free boundaries. This observation could be made rigorous, upon extending the idea in [20], provided pointwise *a posteriori* error estimates were available. This is under further investigation.

REFERENCES

- [1] W. Bangerth and R. Rannacher, *Adaptive Finite Element Methods for Differential Equations*. Lectures in Mathematics ETH Zürich, Birkhäuser Verlag (2003).
- [2] A. Bergam, C. Bernardi and Z. Mghazli, A posteriori analysis of the finite element discretization of some parabolic equations. *Math. Comp.* **74** (2005) 1117–1138 (electronic).
- [3] F. Black and M. Scholes, The pricing of options and corporate liabilities. *J. Polit. Econ.* **81** (1973) 637–659.
- [4] H. Brézis, *Opérateurs maximaux monotones et semi-groupes de contraction dans les espaces de Hilbert*. North Holland (1973).
- [5] H. Brézis and F.E. Browder, Nonlinear integral equations and systems of Hammerstein type. *Adv. Math.* **18** (1975) 115–147.
- [6] M. Broadie and J. Detemple, Recent advances in numerical methods for pricing derivative securities, in *Numerical Methods in Finance*, L.C.G. Rogers and D. Talay Eds., Cambridge University Press (1997) 43–66.
- [7] L.A. Caffarelli, The regularity of monotone maps of finite compression. *Comm. Pure Appl. Math.* **50** (1997) 563–591.
- [8] Z. Chen and R.H. Nochetto, Residual type a posteriori error estimates for elliptic obstacle problems. *Numer. Math.* **84** (2000) 527–548.
- [9] C.W. Cryer, *Successive overrelaxation methods for solving linear complementarity problems arising from free boundary problems*, Free boundary problems I, Ist. Naz. Alta Mat. Francesco Severi (1980) 109–131.
- [10] A. Fetter, L^∞ -error estimate for an approximation of a parabolic variational inequality. *Numer. Math.* **50** (1987) 57–565.
- [11] F. Fierro and A. Veese, A posteriori error estimators for regularized total variation of characteristic functions. *SIAM J. Numer. Anal.* **41** (2003) 2032–2055.
- [12] R. Glowinski, *Numerical methods for nonlinear variational problems*. Springer series in computational physics, Springer-Verlag (1984).
- [13] P. Jaillet, D. Lamberton and B. Lapeyre, Variational inequalities and the pricing of American options. *Acta Appl. Math.* **21** (1990) 263–289.
- [14] C. Johnson, Convergence estimate for an approximation of a parabolic variational inequality. *SIAM J. Numer. Anal.* **13** (1976) 599–606.
- [15] D. Lamberton and B. Lapeyre, *Introduction to stochastic calculus applied to finance*. Springer (1996).
- [16] R.H. Nochetto and C.-S. Zhang, *Adaptive mesh refinement for evolution obstacle problems* (in preparation).
- [17] R.H. Nochetto, G. Savaré and C. Verdi, Error control for nonlinear evolution equations. *C.R. Acad. Sci. Paris Ser. I* **326** (1998) 1437–1442.
- [18] R.H. Nochetto, G. Savaré and C. Verdi, *A posteriori* error estimates for variable time-step discretizations of nonlinear evolution equations. *Comm. Pure Appl. Math.* **53** (2000) 525–589.
- [19] R.H. Nochetto, K.G. Siebert and A. Veese, Pointwise a posteriori error control for elliptic obstacle problems. *Numer. Math.* **95** (2003) 163–195.
- [20] R.H. Nochetto, K.G. Siebert and A. Veese, Fully localized a posteriori error estimators and barrier sets for contact problems. *SIAM J. Numer. Anal.* **42** (2005) 2118–2135.
- [21] M. Picasso, Adaptive finite elements for a linear parabolic problem. *Comput. Methods Appl. Mech. Engrg.* **167** (1998) 223–237.
- [22] A. Schmidt and K.G. Siebert, *Design of adaptive finite element software: the finite element toolbox ALBERTA*. Lecture Notes in Computational Science and Engineering, Springer (2005).
- [23] A. Veese, Efficient and reliable a posteriori error estimators for elliptic obstacle problems. *SIAM J. Numer. Anal.* **39** (2001) 146–167.
- [24] R. Verfürth, *A review of a posteriori error estimation and adaptive mesh-refinement techniques*. Wiley Teubner (1996).
- [25] R. Verfürth, *A posteriori* error estimates for finite element discretizations of the heat equation. *Calcolo* **40** (2003) 195–212.
- [26] T. von Petersdorff and C. Schwab, Numerical solution of parabolic equations in high dimensions. *ESAIM: M2AN* **38** (2004) 93–127.
- [27] C. Vuik, An L^2 -error estimate for an approximation of the solution of a parabolic variational inequality. *Numer. Math.* **57** (1990) 453–471.
- [28] P. Wilmott, J. Dewynne, and S. Howison, *Option Pricing: Mathematical Models and Computation*. Oxford Financial Press, Oxford, UK (1993).